FHWA-AK-RD-84-13

FROST JACKING FORCES ON H AND PIPE PILES EMBEDDED IN FAIRBANKS SILT

Interim Report

By

J.B. Johnson

Cold Regions Research
and Engineering Laboratory (CRREL)

March 1984

Prepared for:

STATE OF ALASKA
DEPARTMENT OF TRANSPORTATION AND PUBLIC FACILITIES
DIVISION OF PLANNING AND PROGRAMMING
RESEARCH SECTION
2301 Peger Road
Fairbanks, Alaska 99701

1. Report No.	2. Government Accession No.	3. Recipient's Catalog No.
AK-RD-84-13		

4. Title and Subtitle	5. Report Date
Frost Jacking Forces on H and Pipe Piles Embedded in Fairbanks Silt	March 1984
	6. Performing Organization Code
7. Author(s) Jerry B. Johnson	8. Performing Organization Report No.
9. Performing Organization Name and Address Cold Regions Research and Engineering Laboratories Hanover, NH 03755	10. Work Unit No. (TRAIS)
	11. Contract or Grant No. F29081
12. Sponsoring Agency Name and Address Alaska Department of Transportation and Public Facilities Pouch Z Juneau, AK 99811	13. Type of Report and Period Covered Interim Report
	14. Sponsoring Agency Code

15. Supplementary Notes

Conducted in cooperation with the U.S. Department of Transportation, Federal Highway Administration

16. Abstract

Axial strains caused by frost heaving and the volumetric expansion of near surface soil layers, were measured between 23 November 1982 and 13 April 1983, on two test piles, embedded in Fairbanks. Test piles consisted of a 12" diameter pipe and a 10 x 57 H-pile, instrumented with strain gauges and temperature sensors at 6" intervals. The strain measurements were used to calculate the uplift forces and shear stresses along the pile - soil interfaces to a depth of approximately ten feet. Uplift forces caused by frost heaving were highest following major cold periods. Fluctuation in force levels through the year correlated well with soil temperature fluctuations at depth, but lagged air temperature fluctuations by one or more days. Beginning in February, strong diurnal force fluctuations occurred which were directly correlated with near surface soil temperature fluctuations. These were ascribed to temperature-induced volumetric expansion and contraction of the upper soil layers.

The highest uplift force for the H-pile was 212 kips at a depth of 8 feet, measured on 22 January 1983. The maximum shear stress was 93 psi on the total H-pile surface area, and 152 psi when the H-pile surface area was computed using a rectangular outer boundary geometry for the pile. The maximum force and shear stress for the pipe pile were 158 kips at a depth of 6.8 feet and 130 psi on 18 January 1983.

Water was frozen around each pile in mid-winter to simulate the formation of aufeis around bridge piles. Tangential forces and stresses on the piles were highest during the freezing period and caused a maximum increase in force in the H and pipe piles of about 12 kips and 25 kips above the ambient force levels.

17. Key Words	18. Distribution Statement
Frost Heave, Piles, Pile Friction, Silts, Permafrost, Thermopiles	

19. Security Classif. (of this report)	20. Security Classif. (of this page)	21. No. of Pages	22. Price
Unclassified	Unclassified	80	N/A

PREFACE

This report covers the first year of observations and conclusions on two instrumented frost heave test piles installed in Fairbanks silt. These pilings were again monitored for temperatures, heave stresses, and heave rates of surrounding soils during the 1983-84 winter, with a layer of compacted sand and gravel placed around the piling; and a second year report summary is scheduled for late 1984. Observations may also be conducted during the 1984-85 winter with further soil replacement used to analyze the heaving stresses generated by different soil types. A thick ice collar around the tops of the piles is also planned, to simulate the gripping action of river ice on piling.

The test piling installed for use in this study have provided a very valuable facility for analyzing the frost heave stresses on piles in seasonal frost zones. The use of passive heat-pipes or "thermo-siphons" to refrigerate and anchor the lower ends of these test piles in permafrost without significant uplift, in spite of jacking forces exceeding 100 tons, has also served to demonstrate the capability of such devices in creating a stable anchorage for foundations in permafrost.

David C. Esch, P.E.
Highway Research Manager
Department of Transportation
and Public Facilities

TABLE OF CONTENTS

ABSTRACT

Axial strains caused by frost heaving and the volumetric expansion of near surface soil layers, were measured between 23 November 1982 and 13 April 1983, on two test piles, embedded in Fairbanks. Test piles consisted of a 12" diameter pipe and a 10 x 57 H-pile, instrumented with strain gauges and temperature sensors at 6" intervals. The strain measurements were used to calculate the uplift forces and shear stresses along the pile - soil interfaces to a depth of approximately ten feet. Uplift forces caused by frost heaving were highest following major cold periods. Fluctuation in force levels through the year correlated well with soil temperature fluctuations at depth, but lagged air temperature fluctuations by one or more days. Beginning in February, strong diurnal force fluctuations occurred which were directly correlated with near surface soil temperature fluctuations. These were ascribed to temperature-induced volumetric expansion and contraction of the upper soil layers.

The highest uplift force for the H-pile was 212 kips at a depth of 8 feet, measured on 22 January 1983. The maximum shear stress was 93 psi on the total H-pile surface area, and 152 psi when the H-pile surface area was computed using a rectangular outer boundary geometry for the pile. The maximum force and shear stress for the pipe pile were 158 kips at a depth of 6.8 feet and 130 psi on 18 January 1983.

Water was frozen around each pile in mid-winter to simulate the formation of aufeis around bridge piles. Tangential forces and stresses on the piles were highest during the freezing period and caused a maximum increase in force in the H and pipe piles of about 12 kips and 25 kips above the ambient force levels. Once the water was frozen, force and stress levels in the piles returned to levels caused by frost heaving only.

ACKNOWLEDGEMENT

The help and cooperation of many individuals was required to complete this study. I would especially like to express my appreciation to Mr. Dave Esch for his help in developing the technical program and providing logistical support throughout the project. The assistance of the Cold Regions Research and Engineering Laboratory in installing the piles is acknowledged. Mr. D. Haynes and Mr. D. Dinwoodie were especially helpful. I would also like to express my gratitude to Mr. Dan Solie for his assistance in instrumenting and installing equipment during the study and his help in analyzing the data. This work could not have been completed without the efforts of Messrs. W. Zito, M. Sturm, C. Olmsted, L. Kozycki and R. Briggs.

This report was reviewed technically by Mr. D. Esch and Mr. F. Crory. Funding was provided by the Alaska Department of Transportation and Public Facilities.

LIST OF FIGURES

LIST OF FIGURES (CONT.)

LIST OF FIGURES (CONT.)

LIST OF FIGURES (CONT.)

LIST OF FIGURES (CONT.)

LIST OF TABLES

SUMMARY AND CONCLUSIONS

Axial strain measurements were used to calculate the magnitude and distribution of axial stresses in an H-pile and a pipe pile resulting from frost heaving and temperature induced volumetric changes in the soil. The axial stresses were then used to calculate the vertical forces acting at the pile surface - soil interface. The forces were used to calculate the shear stresses that act on the outer skin of the piles, which may be caused by adfreezing of the soil or soil friction. Strain gauges and thermocouples were placed every six inches along the upper ten feet of the 31 foot length of both piles. The piles were installed into dry augered holes to a depth of approximately 29.5 feet in late October. Heat siphons were used to freeze the backfill material and increase the bond between the soil and piles at depth. Temperature logging tubes were installed next to the piles and logged twice during the experiment to examine the effectiveness of the heat siphons at removing heat from the soil. These measurements indicated that the heat siphons did cool the soil at depth and that the siphon in the pipe pile was more effective than the siphon in the H-pile. A string of thermistors was installed near the piles to monitor ground temperatures. Soil surface heave measurements were made monthly using standard levelling methods. A benchmark protected from frost heave was used as a reference and eleven survey markers along with the piles constituted the survey net. In mid-January, four markers were covered with ice and the remaining seven were surveyed for the rest of the year. Pile strains and temperatures, soil temperatures and air temperature measurements were taken at regular time intervals that varied from two to six hours from late November 1982 through early April 1983. The magnitudes of strains, forces and shear stresses reported in this study represent lower bounds to the actual values since voltage measurements used as the reference to calculate strains were obtained after soil freezing was well advanced. In mid-January, water was frozen around each pile in an effort to simulate the effects of aufeis formation around bridge piers.

The principal findings of the study were that:

1. The highest rate of soil surface heave occurred from November through December and gradually decreased throughout the winter,

2. The total average accumulated heave from November through March was 0.126 feet,

3. Maximum frost heave forces and shear stresses were associated with the five major cold cycles that occurred during the experiment,

4. Fluctuations in force and shear stress levels were correlated with soil temperature fluctuations at depth and lagged air temperature fluctuations by one or more days,

5. The maximum force and shear stress for the H-pile were 212 kips at 8 feet and 93 psi on 22 January 1983; the maximum shear stress was 152 psi when the H-pile surface area was computed using a rectangular outer boundary for the pile,

6. The maximum force and shear stress for the pipe pile was 158 kips at a depth of 6.8 feet and 130 psi on 18 January 1983,

7. Average shear stresses for the H and pipe piles, to the depth of the peak forces were 24 psi and 47 psi respectively; the average shear stress for the H-pile was 39 psi when the H-pile surface area was computed using a rectangular outer boundary for the pile,

8. The freezing of water around the piles resulted in sudden large increases in the forces in the piles which may be related to temperature induced volumetric changes in the ice or near surface soil layers,

9. The maximum change in forces associated with freezing water around the H and pipe piles were 12 kips and 25 kips respectively,

10. Once the water had frozen around the piles the measured forces and stresses caused by the ice blocks dropped to ambient levels associated with the frozen soil,

11. The direction of shear stresses fluctuated between positive (upwardly directed) and negative (downwardly directed) causing fluctuations in the magnitude of forces, along the vertical surface of each pile,

12. Strong diurnal temperature changes caused diurnal force fluctuations in the piles that may be due to temperature induced volumetric expansion of the upper soil layer,

13. The force and shear stress levels for the pipe and H-piles were of similar magnitudes with fluctuations in force levels for the H-pile tending to be smoother and less dramatic than for the pipe pile,

14. The observed forces acting on the piles may be explained by temperature induced changes in heave rate, soil adfreeze strength, and by volumetric changes in near surface soil layers.

RECOMMENDATIONS FOR FUTURE RESEARCH

The measurement and data analysis program for the frostjacking study during the 1982-1983 winter was successful. However, there are a number of modifications to the experiment that would help to increase our understanding of frostjacking forces on foundation piles. These include:

1. Continuing the measurement program through the summer (1983) and winter (1983-1984) to provide reference strain readings and data for one complete freezing cycle,

2. Installing linear variable differential transformers (LVDT's) to measure soil surface heave more frequently and accurately than was possible using standard surveying methods,

3. Installing an open air snow shelter over the experimental site,

4. Installing a second power line to the instrumentation hut to provide a stable power source for instruments,

5. Conducting a time series spectral analysis on the LVDT soil heave data, strain measurements and soil temperature profiles to develop a relationship between heave force, soil heaving and soil temperature fluctuations.

6. Recalibrate piles after experiment.

FROST HEAVE FORCES ON PIPE AND H PILE

Introduction

Foundations embedded in frost susceptible soils can be subjected to large uplift forces resulting from frost heaving of soils. These forces can cause an upward vertical displacement of foundations which are not embedded below the frost depth or do not have sufficient resistance to heaving forces. Frost heave damage to buildings, roadway and railroad bridges, utility poles and other permanent structures are well documented (Pe'we, 1982; Domaschuk, 1982). In Alaska, H and pipe piles are often used to support light buildings and bridges. It is important that design engineers know the magnitude of frost heaving forces that can act on foundation piles and how these forces are distributed along the piles. This information is used to determine the depth to which a pile needs to be embedded to resist heaving forces and the tensile strength requirements of a pile. This study was designed to measure the magnitude and distribution of the axial strains in an H pile and a pipe pile embedded in Fairbanks silt. Once the strains are known the forces acting on the piles and the shear stresses at the pile-soil interface are calculated. These results will provide complete force and stress information on the piles as they are subjected to frost heaving. In general, previous studies have provided data on only the total load acting on pipe piles due to frost heaving.

The results of this study provides new information on the magnitude and distribution of frost heaving forces on H and pipe piles. The results will also add to the information base that Alaska Department of Transportation personnel utilize when designing pile foundations to resist frost heaving forces.

Summary of Previous Research:

Studies of the uplift forces induced by frost heaving of foundations date back to early Russian work in the 1930's reported by Tsytovich (1975). Direct measurements of frost heave forces were made in Russia from 1958 - 1963. Three methods were used to measure frost heave forces; (1) reaction beam and load cell, (2) force balance apparatus, and (3) electric strain gauges. The reaction beam device consisted of a reaction beam held in place with rods anchored into the soil depth. The test pile was restrained from moving by the beam and the uplift forces acting on the pipe were measured with a load cell placed between the beam and pile. In the force balance scheme, any vertical displacement of the test pile was compensated by an additional load. The load that just stopped the heaving of the pile completely during the freezing of the soil was taken as the maximum total heave force. Additional frost heave measurements were made using strain gauges mounted to the inner surface of a tubular pile. These showed that the relative heaving force acting on the pile was zero at the soil surface, then reached a maximum at some depth between the soil surface and 0°C isotherm and decreased to zero at the 0°C isotherm. The maximum of the heaving forces shifted downward toward the freezing boundary as the frost depth increased and the shear stresses acting along the pile soil interface increased along the pile length with decreasing soil temperature (Tsytovich, 1975). The results for the strain gauged pipe are of interest because of the similarity to the test setup in this study. They indicate that the uplift forces (due to frost heaving) and restraining forces are not uniform along the length of the pile. Figure 1 shows the forces per lineal cm acting on the pile with respect to depth. The proper interpretation for these results is that the uplift shear stresses due to heaving act from the soil surface to the maximum force value. The restraining forces act from the maximum force value downward until the uplift forces are matched. In all cases the uplift forces were counteracted by restraining forces before the depth of the 0°C isotherm was reached. These results differ from the usual concept of how heaving forces act on piles. The common description of heaving is that the shear stress due to heaving act from the soil surface to the freezing front which is usually

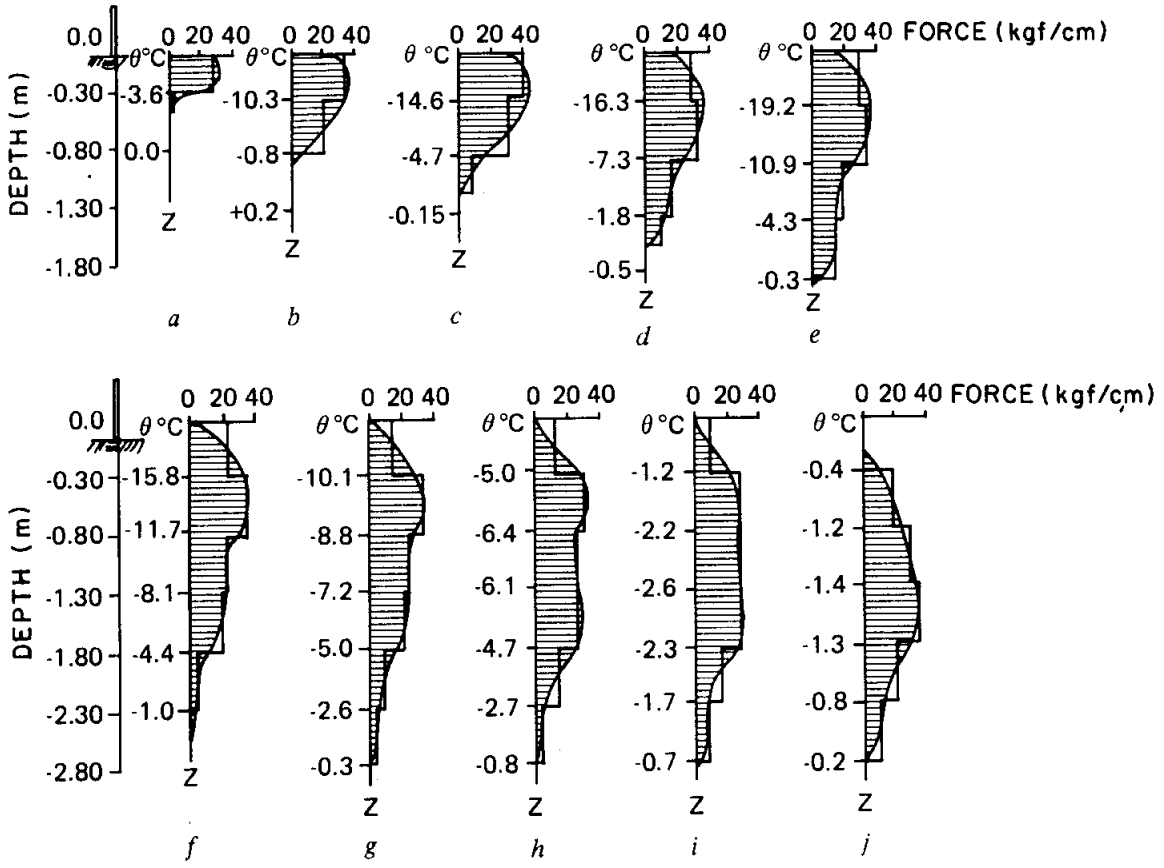

Figure 1. Distribution of relative frost-heaving forces, τ_z, in kgf/cm, over the lateral surface of the pile (experiments of Yegerev reported by Tsytovich, 1975). (a) 4 Nov 1957; (b) 14 Nov 1957; (c) 25 Nov 1957; (d) 28 Dec 1957; (e) 11 Jan 1958; (f) 11 Mar 1958; (g) 16 Apr 1958; (h) 5 May 1958; (i) 26 May 1958; (j) 11 June 1958; z is depth in meters from the surface and θ° is the temperature in degrees Celsius. Conversion to English units can be done by using 2.2 lb = 1 kgf, 1 in. = 2.54 cm, and 3.281 ft = 1 m.

taken to be 0°C. The restraining forces act from the 0°C isotherm downward. There is not sufficient information about the setup or procedures for the Russian experiment to make an accurate comparison to other available experimental results.

Additional field measurements of frost heaving forces on piles have been conducted in Japan, the United States and Canada (Kinosito and Ono, 1963; Crory and Reed, 1965; Penner and Irwin, 1969; Penner and Gold, 1971; Penner, 1974 and Domaschuk, 1982). These have consisted of reaction beam and load cell tests. One test was conducted using a strain gauged pile; however the results of the test are not available to the author. Crory and Reed (1965) reported the results of frost heaving force measurements conducted from 1956 to 1963 on 8 inch standard steel pipe and 13-15 inch butt diameter creosoted timber piles. The piles were embedded into silty soils overlying permafrost at the U.S.A. CRREL Fairbanks field station. The site conditions were very similar to those of the current study which was located at the USA CRREL field station. Air temperature, soil temperature, heaving of an unrestrained pile, heaving of the test pile, and the heave force were measured during the winters of 1956-1957, 1957-1958 and 1962-1963. The forces observed in the first two tests (1956-1967 and 1957-1958) were below the maximum forces which might have been generated. The skin friction between the reaction beam support piles and permafrost was not sufficient to resist heaving during the 1956-1957 test and the soil was exceptionally dry during the 1957-1958 test. Distinct fluctuations in the heave force measurements were observed for both steel and timber piles. The maximums and minimums of the fluctuations occurred a few days after a respective decrease or increase in air and soil temperatures (Crory and Reed, 1965).

Canadian experiments measured heaving forces of wood, steel, and concrete columns, from 3 inches to 12 inches in diameter, embedded into Leda clay (Penner and Irwin, 1969; Penner and Gold, 1971 and Penner, 1974). The shear stresses due to heaving were highest for steel, followed by concrete and wood. This was mostly attributed to the influence of temperature on the adfreeze strength of frozen soil. The steel columns were normally colder than the concrete or wood columns. Domaschuk (1982)

conducted controlled heaving tests of steel structural units. Tests were conducted on embedded vertical steel members and steel members inclined to the soil surface. The test results indicated a decrease in vertical stress on the member as the angle of inclination of the member with respect to the frost plane increased. Kinosita and Ono (1963) conducted frost heave force measurement tests on steel, concrete, resin coated concrete and vinyl columns. These tests indicated that adfreeze strength was the greatest for steel and was less for vinyl and wood. The Canadian and Japanese experiments both showed the fluctuations in heave force associated with changes in the air temperature that had been observed by Crory and Reed (1965). These were attributed to changes in ground temperature and ground temperature gradients caused by air temperature fluctuations. Table I summarizes the measurements of peak averaged uplift shear stress acting along the pile soil interface stress induced by frost heaving where uplift shear stress is defined by the uplift force divided by the surface area of the pile to the depth of the 0°C isotherm.

The above investigators suggested a number of controlling influences for frost heaving forces acting on foundation piles. These included (1) soil temperature, (2) rate and magnitude of soil surface heave, (3) changes in soil temperature, (4) soil temperature gradients and (5) the availability of moisture in the soil. Maximum shear stresses generally occurred during the early freezing period when heaving rates were high. Maximum uplift forces often occurred near the time of maximum frost penetration.

TABLE I

Peak Frost Heaving Stresses Measured on
Steel, Concrete and Wood Piles

Investigators	Soil Type	Year of Test	Pile Dimensions (Pile Diameter)	Shear Stress (psi) Steel	Vinyl	Concrete	Wood
Kinosita and Ono, 1983	Silty clay loam	1961-62	2.83 in	30			
			3.0 in		23.5	16.6 uncoated	
		1961-62	3.7 in			7.4 resin coated	
Crory and Reed, 1965	Silty	1956-57	8.0 in	22			
		1957-58	8.0 in	23			
		1958-59	14.0 in				8.0
		1962-63	14.0 in				12.0
		1962-63	8.0 in	41			
Russian data reported by Tsytovich, 1975	?	1958-63	?				14-24
Penner and Irwin, 1969	Clay	1966-67	3.5 in	12			
		1967-68	3.5 in	12			
Penner and Gold, 1971	Clay	1970	3.5 in	16.5		19.5	13.0
Penner, 1974	Clay	1970-71	3.0 in			16.5	16.8
		1970-71	6.0 in			21.8	25.7
		1970-71	12.0 in			17.3	20.2
		1971-72	3.0 in	37.0		27.9	19.0
		1971-72	6.0 in	29.4		36.1	32.8
		1971-72	12.0 in	25.0		20.4	35.3
Domaschuk, 1982	Silty		3 x 3 in angle	50.0			

METHODS AND MATERIALS

Soil Conditions

The test site was located on the Alaska Department of Transportation and Public Facilities Permafrost Thawing Test Plot D at the U.S.A. CRREL Alaska Field Station (Figure 2). The soil and permafrost conditions at the field station have been described by Crory and Reed (1965), Linell (1973), and Esch (1982). The soils are primarily deep colluvial deposits of slightly organic silts with occasional wood fragments and peat layers. Average particle size analyses indicate that the soil consists of about 85% silt or clay size particles and 15% fine sand size particles (Crory and Reed, 1965; Linell, 1973). Moisture content was not measured in the Fall; however, observation of borehole cuttings indicated that the soil deposits were saturated. Frost heaving of snow covered areas at the site is approximately 1 to 3 inches during a typical winter. The active freezing and thawing depth of the soil is approximately 5 to 6 feet.

Site Preparation and Plan

The experimental site had been cleared of vegetation and covered with a thin layer of gravel during an earlier study. Two instrumented piles, a pipe pile and an H-pile, were installed at the test site. A reference benchmark, temperature probes and an instrumentation hut were also installed (Figure 3). The snow cover was removed from the site just prior to equipment installation; the site was subsequently cleared of snow as required.

Instrumentation and Installation of Piles

An H-pile (10 in. Web, 57 lbs per lineal foot) and a pipe pile (12 in. I.D., 3/8 in. wall thickness) were each instrumented with strain and temperature sensors. Hermetically sealed weldable strain gauges (oriented to measure axial strain) and copper-constantan thermocouples were placed

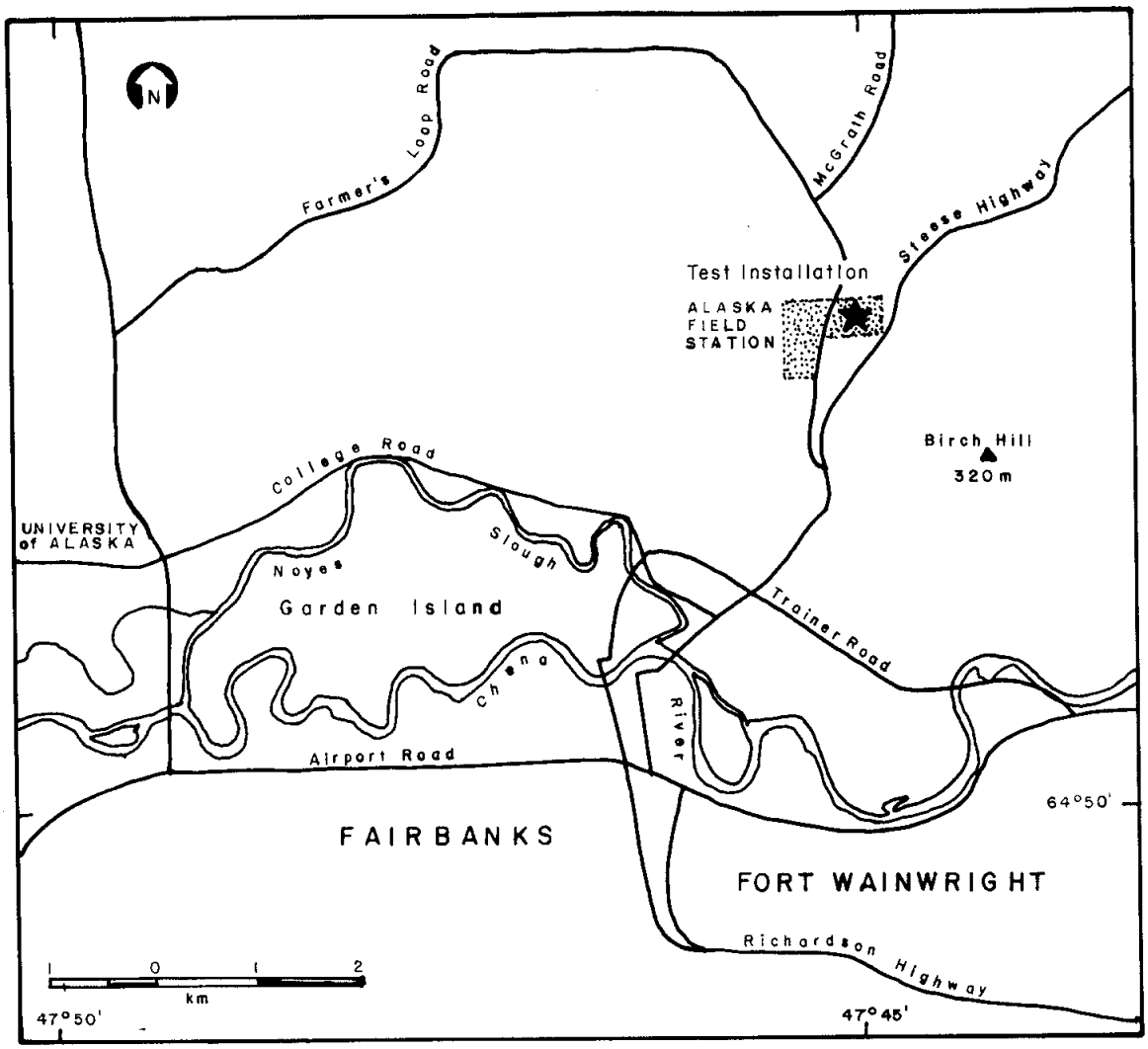

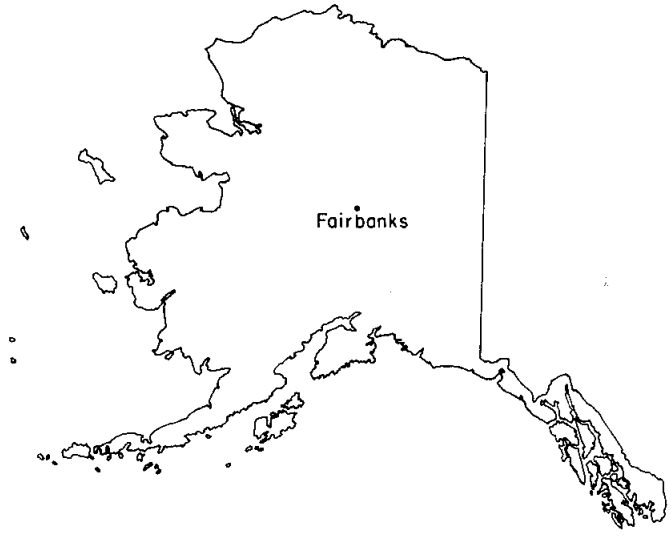

Figure 2. Experiment site location map.

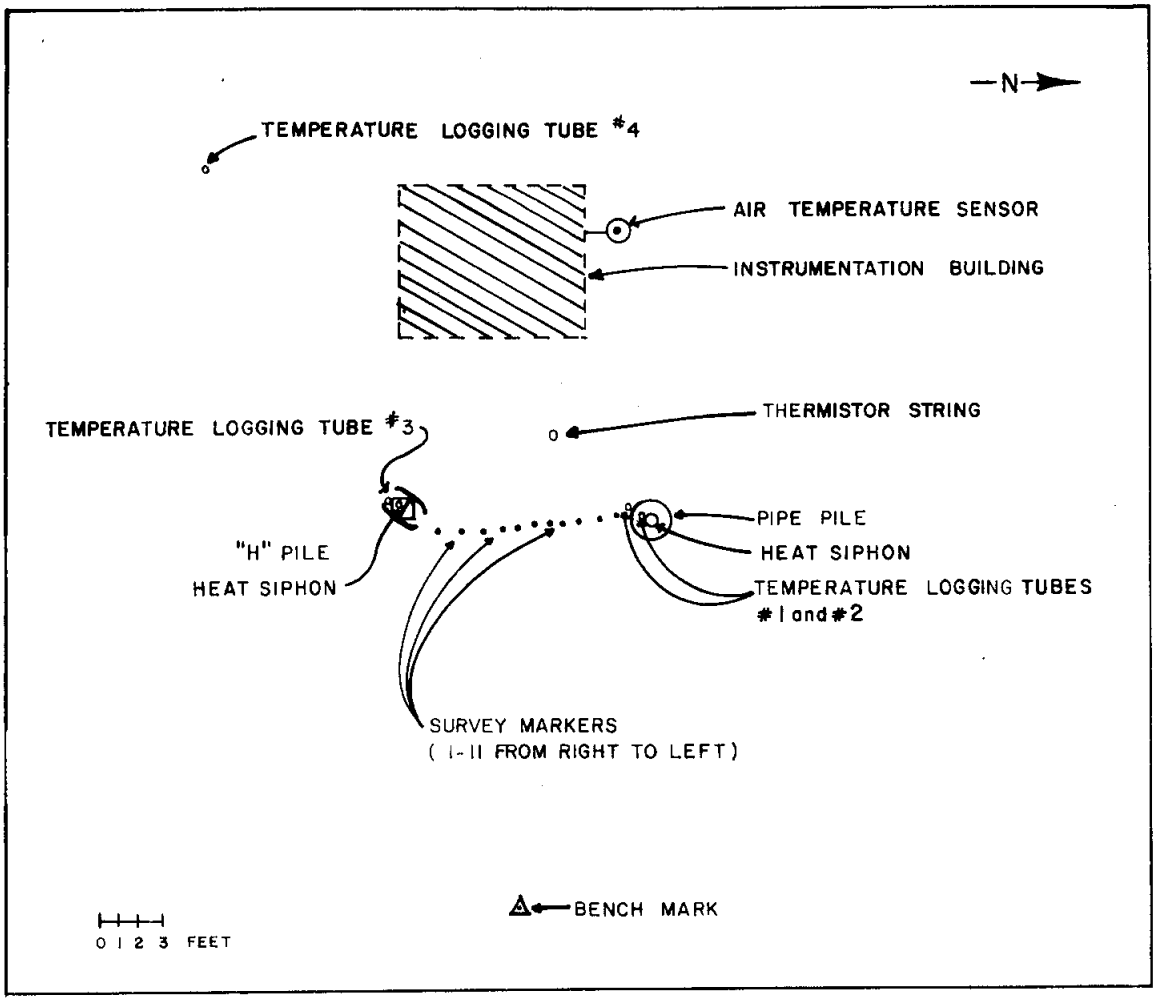

Figure 3. Plan view of the experimental site.

every six inches along the upper ten feet of the 31 ft. length of both piles as shown in Figure 4, 5, 8 and 9. Strain gauges oriented at 90 degrees to the axial direction were interspersed between the axially oriented gauges along the length of the instrumented sections. The gauges were used to measure transverse strains in the piles and to estimate the magnitude of compressive stresses acting on the piles.

Pipe Pile

The pipe pile gauges were placed on diametrically opposite sides of the inside wall of the pipe and were wired to monitor average axial strain, hoop strains and temperature induced apparent strain. The upper nine feet of the pile had been cut into three 36 inch long sections to facilitate instrumentation.

Temperature induced apparent strains were measured using a strain gauge mounted on a metal shim with the same thermal expansion properties as the pile and then fixing one end of the shim to the pile to ensure that the gauge-shim system was unstressed (shown as dummy gauges in Figure 4). In some cases gauges mounted on metal shims were wired to active gauges to cancel temperature induced apparent strains (shown as pairs of gauges in Figure 4).

In other cases single gauges were mounted either directly to the pile to measure transverse strains or on metal shims to measure temperature induced apparent strains. These are shown as single gauges oriented at 90 degrees to the axial direction of the piles. Figure 6 shows a close up of one of the strain gauge installations including the active gauge (T) the temperature compensation gauge (C) and the thermocouple. The potted object labeled 6 in the figure provides for strain relief and environmental protection for the wire connections. After installation all gauges were covered with a waterproof electrical coating to reduce corrosion of the metal around the gauges. The instrumented pile sections were welded back together, calibrated and then welded to the lower uninstrumented section of pile. The gauges were kept cool during welding by blowing a stream of air through the pile and running water over the outer skin. Concentric rings were welded to the lower section of the pile to help prevent the pile from heaving throughout the winter period (Long, 1972).

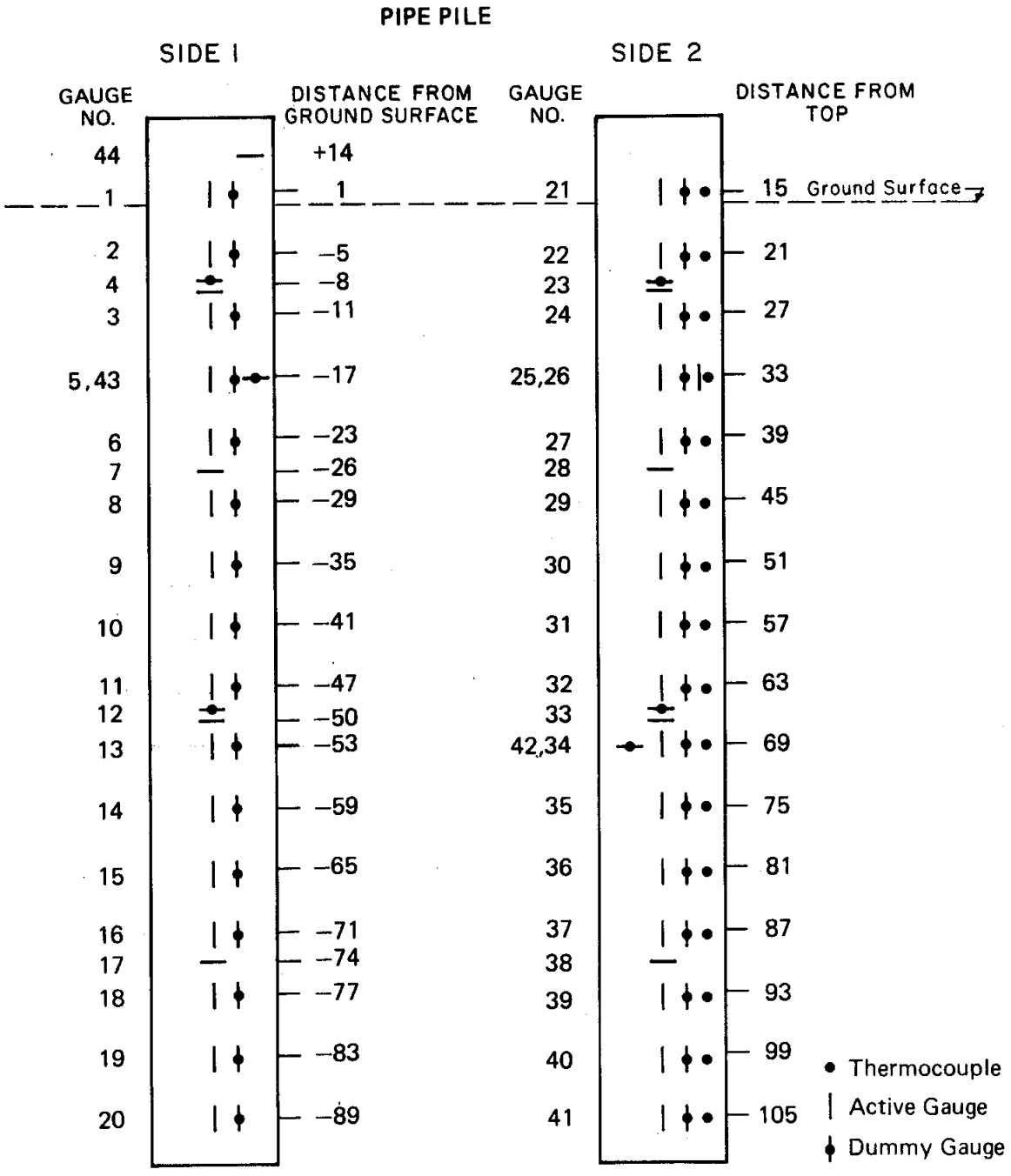

Figure 4. Layout pattern for strain gauges and thermocouples for the pipe pile.

Figure 5. End view of a strain gauge and thermocouple-instrumented 3-ft-long pipe pile section.

Figure 6. Close-up view of a strain gauge and thermocouple installation for the pipe pile.

Two tubes were placed in the interior of the pile. One tube was suspended in the center of the pile as a guide for a heat siphon. The second tube was slightly offset from the center and was used to pour a slurry of water and sand into the base of the pile after installation. Once both tubes were in place, polyurethane foam was used to fill the upper 9 ft. cavity of the pile (Figure 7).

H-Pile Instrumentation

Instrumentation of the H-pile was similar to that of the pipe pile. Figure 8 shows the locations of the strain gauges and thermocouples along the length of the pile. The active strain gauges and thermocouples were attached along the centerline of each side of the H-pile web and two five inch angle covers were welded over the gauges to provide mechanical protection. Active and temperature compensation gauges were wired in pairs to compensate for temperature induced apparent strains. Figure 9 shows the installation scheme for two axially-oriented and one transverse strain gauge with a thermocouple installed next to each of the axial gauges. An 11 ft. tube was placed inside of the angle on side 1 and connected to a 4 inch water-tight box section used as a guide and housing for a thermal cooling probe that extended for the remaining length of the pile. Polyurethane foam was used to fill the cavity in the angles for the length of the instrumented section. Frost heave resistance was obtained through plates welded to the base section of the pile (Figure 10).

Both piles were calibrated in compression over the range 0-10,000 lbs (a description of the calibration procedures and results is given in Appendix B). The piles were then installed in 20 inch dry augered holes at the experimental site. The calibration tests were used to establish the effective Young's modulus for the piles and to detect flawed gauges. The piles were set into the predrilled holes to a depth of approximately 29.5 feet leaving the upper 15 inches of each pile exposed above ground. Propane filled heat siphons were inserted into the guide tubes of each pile. A slurry of sand and water was poured into the lower 10 feet of the pipe pile to increase the thermal contact between the heat siphon and the soil

Figure 7. Instrumented pipe pile after welding of the three instrumented sections to the uninstrumented section and installation of the polyurethane foam.

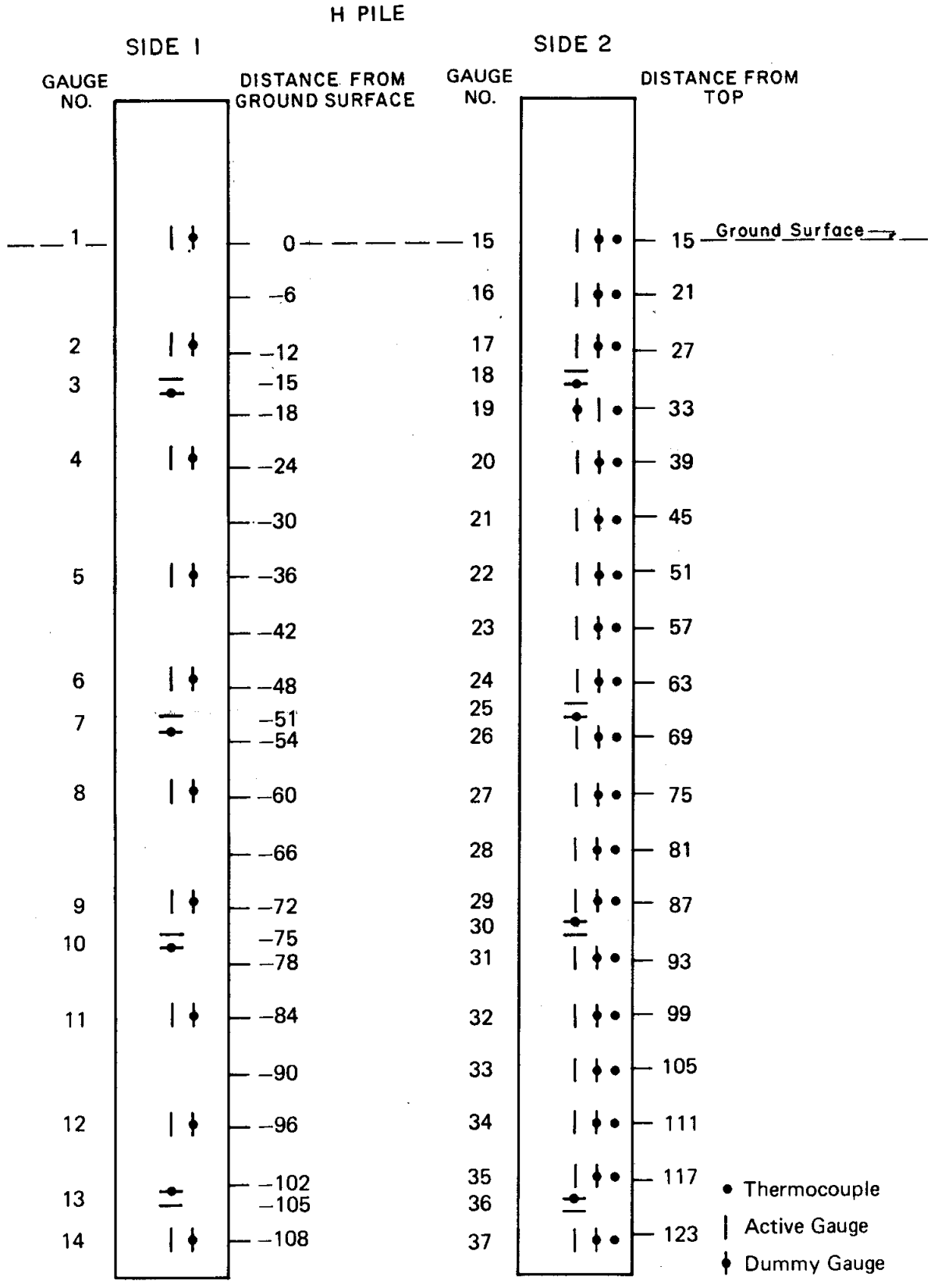

Figure 8. Layout pattern for strain gauges and thermocouples for the H-pile.

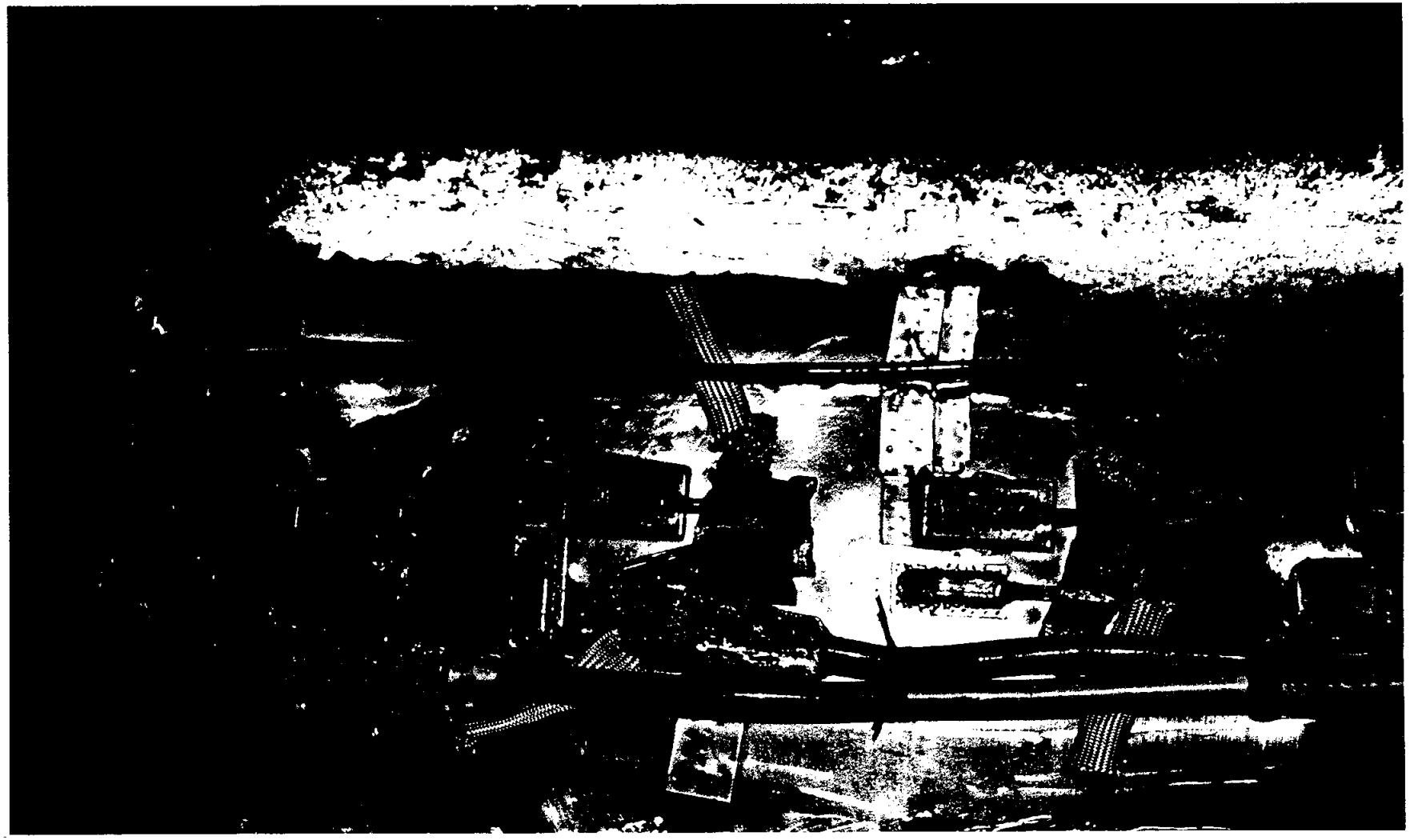

Figure 9. Close-up view of axial and transverse strain gauge and thermocouple installations on the H-pile.

Figure 10. Instrumented H-pile after installation of protective angles, guide tube and retention bars.

surrounding the pile. No thermal contacting agent was added to the H-pile. The heat siphons were installed to aid in freezing the backfill slurry around the piles and to cool the permafrost at depth, increasing the jacking resistance of the piles in combination with the rings and plates welded on for the same purpose. Insulation surrounded the upper sections of the thermal cooling probes in the H-pile and pile pile. This helped reduce air cooling of the piles and radial freezing of the soil which might have reduced heave stresses. Three 20 foot temperature logging tubes were installed around the piles to monitor the effectiveness of the heat siphons. The test pile auger holes were backfilled with a slurry of water and sand for the lower 20 feet and with native silt for the upper 10 feet during the week of 31 October 1982. An effort was made to maintain a 40% moisture content for the silt. The effectiveness of the heat siphons at cooling the back-fill soil can be seen from Figure 11 and 12. Temperature readings were taken in the logging tubes near the piles and for the undisturbed soil on two different occasions. Tubes #1 and #2 for the pipe pile were located outside the pile at 10 inches, and inside the pile at about 2½ inches from the heat siphon. Tube #3, for the H-pile, was located about 11½ inches from the heat siphon and Tube #4 was located 10 feet from the H-pile (Figure 3). Figure 11 shows that the soil at depth immediately surrounding the pile was significantly cooler than the undisturbed soil on 7 December and continued to cool throughout the winter. Figure 12 shows that the soil around the H-pile at depth was cooler than the undisturbed soil. The effectiveness of the cooling probe for the H-pile was less than that used in the pipe pile. This may have been due to a lack of good thermal contact between the H-pile and cooling probe.

Temperature Measurements

Temperatures of the soil, piles and air were measured on a regular basis throughout the study. Soil temperatures were measured at six inch intervals from the surface to a depth of 9 feet using a string of Fenwal UUA33J1 curve matched thermistors. The thermistors were suspended in a glycol filled PVC tube that had been inserted into the ground. Temperatures along approximately the upper 10 feet of the piles were measured using copper-constantan thermocouples. Air temperature measurements were made using a copper-constantan thermocouple mounted in a protective housing on the north side of the instrumentation hut.

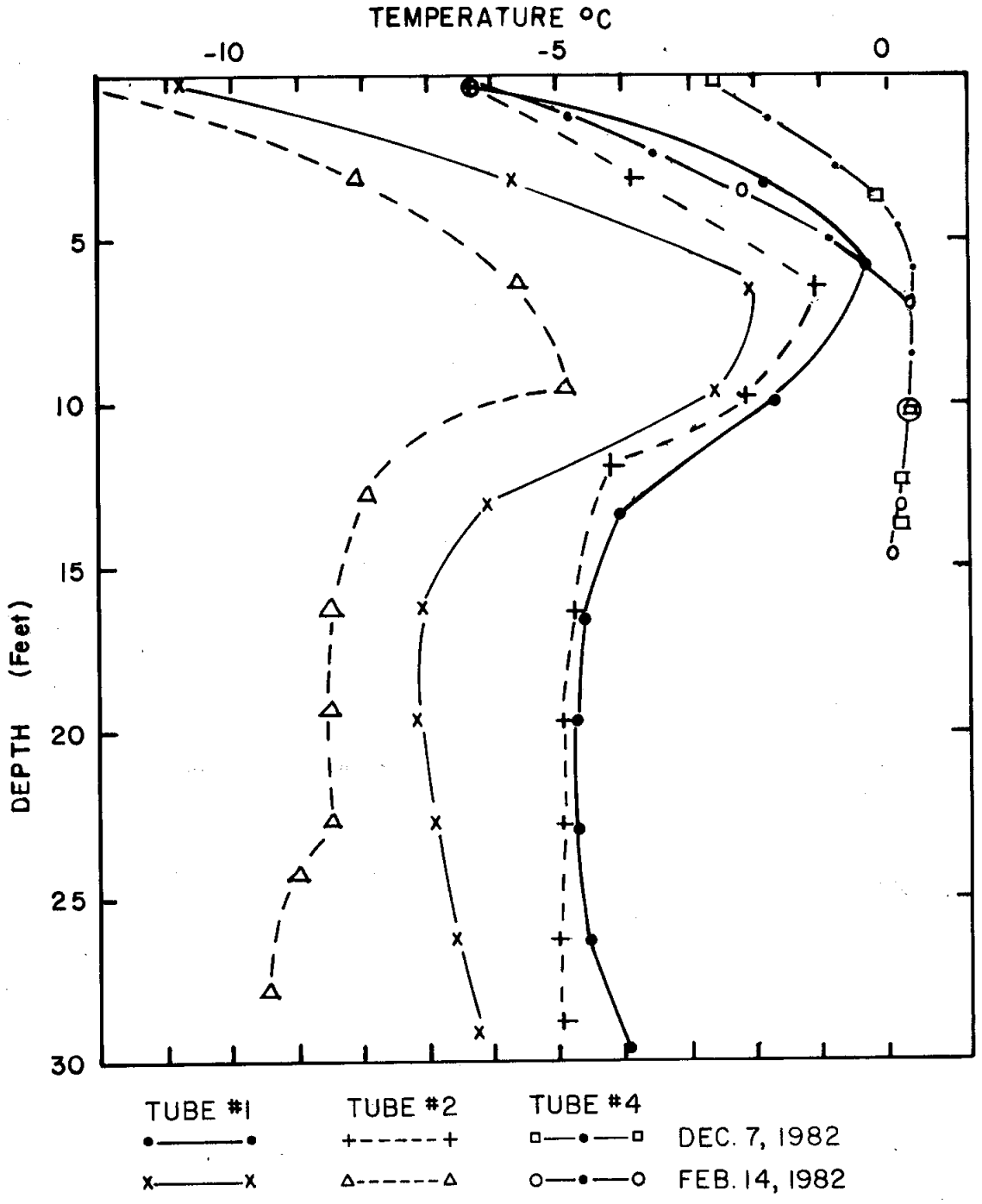

Figure 11. Temperature profiles in the vicinity of the pipe pile and in undisturbed soil. Tube #1 was located outside the pile about 10 inches from the heat siphon, Tube #2 was located inside the pile at 2½ inches from the heat siphon, and Tube #4 was located about 20 feet from the experimental site.

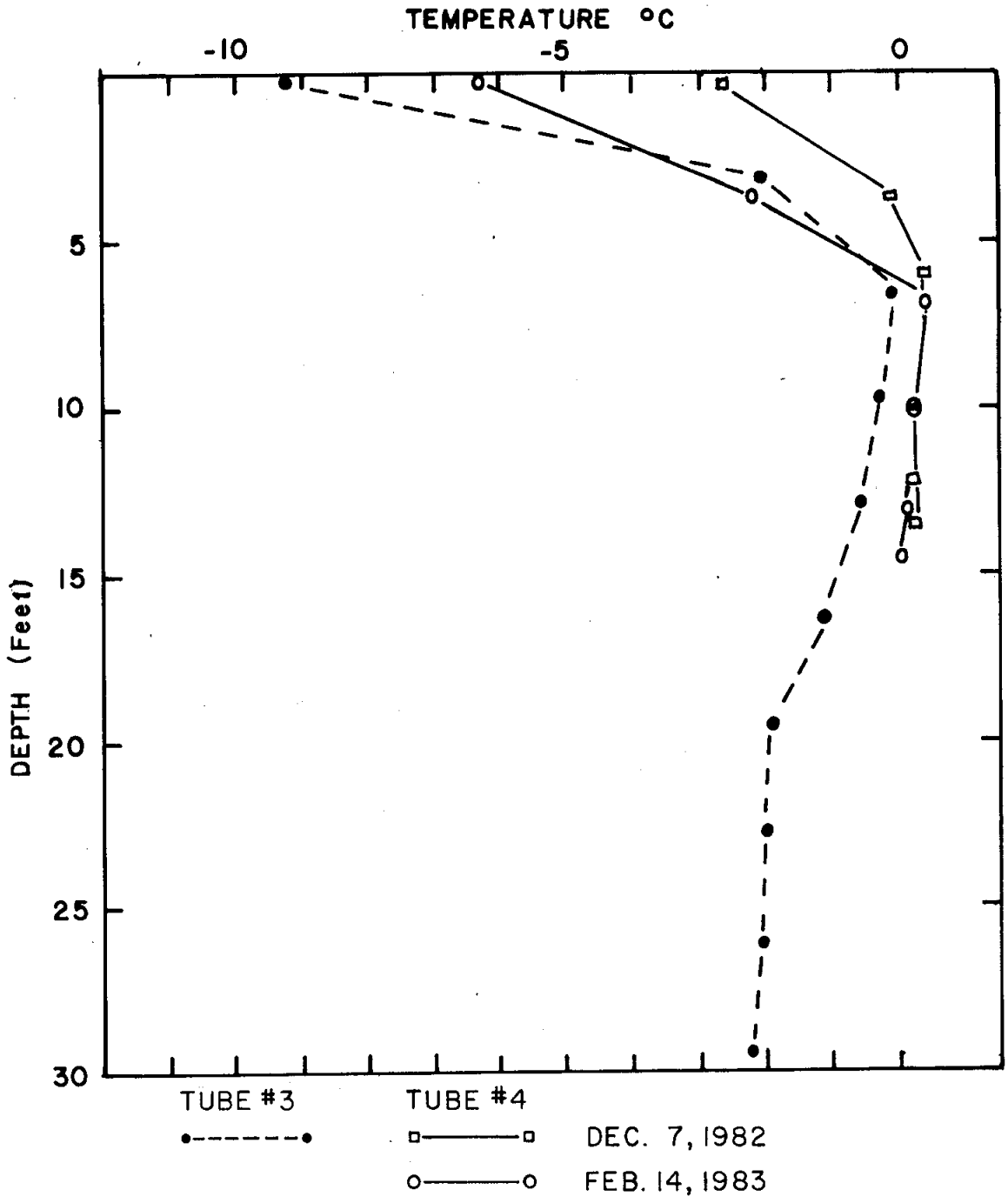

Figure 12. Soil temperature profile near the H-pile. Tube #3 was about 11½ in. from the heat siphon and tube #4, undisturbed soil, was about 20 ft from the experimental site.

Surveys

Standard leveling practices were used to determine changes in elevation of the piles and of several intermediate survey markers between the piles as shown in Figure 3. These observations were made monthly, with differences in elevation between surveys being determined to an accuracy of ± .04 inches. A reference benchmark was placed adjacent to the test site in an area that had approximately 2 feet of active freezing and thawing soil above the permafrost. The benchmark was prevented from heaving by installing a 1 inch by 10 foot pipe with an oversized pointed tip on its base into a 2 inch diameter by 5 foot cased hole. The 1 inch pipe was driven into the permafrost to a depth of approximately 9 feet and the annulus between the pipe and casing was filled with a non-freezing fluid. Each survey marker consisted of a spike driven through a 6 inch square of plywood into the ground. The head of the spike constituted the level point and leveling data were the averages of five closed level loops.

DISCUSSION AND RESULTS

Introduction

The H and pipe piles were installed on 29 October 1982, and routine data acquisition began on 19 November after the installation of the instrument hut, electrical power and connection of all strain and temperature sensors to the HP 3497A. The ground temperatures away from the piles were essentially at or below 0°C at all depths in the soil layer above the permafrost by 19 November. Consequently, strain measurements referenced from the initial readings taken on 19 November would have underestimated the net strains caused by heaving. In an effort to establish a reference for subsequent strain readings, both piles were thawed to an approximate depth of 20 inches on 23 November 1982. The strain gauge output voltage readings taken after the pile temperatures stabilized were used as the reference readings for all subsequent measurements. Even these reference voltage readings did not provide a true reference since the

active freeze-thaw soil layer surrounding the pile was frozen prior to beginning data acquisition. The strains measured in this study do not represent the absolute or maximum strains in the piles caused by heaving because the reference voltages were not determined prior to the start of heaving. The results presented in the following therefore represent only a lower bound to the actual strains, tangential forces and shear stresses acting on the piles.

Vertical Displacement of the Soil and Piles

The eleven survey markers set onto the surface of the soil were used to profile the vertical displacement of the soil between the piles (Figure 3). Only one set of displacement measurements were taken using all survey markers. These measurements were not sufficient to determine the influence of the foundation piles on the soil surface displacement profile. Survey markers 1, 2, 10 and 11 were intentionally covered with ice on 10 January 1983 and subsequent attempts to obtain accurate data from these points was unsuccessful. The vertical displacements for markers 3 through 9 were used to determine the average incremental and accumulated vertical displacement for the soil surface throughout the experiment (Figure 13). The largest measured incremental vertical displacement occurred between November and December; later incremental displacements steadily decreased throughout the winter. This is reflected in the average accumulated vertical displacement for the soil surface. Figure 13 also shows the vertical displacements for the H and pipe piles during the winter. It is apparent that neither the H or pipe pile heaved during the experiment, at least within the resolution of the survey methods (± 0.04 inches).

Forces and Shear Stresses

Strain and temperature measurements were routinely taken at intervals of between two and six hours from 23 November 1982 to 13 April 1983. Such frequent measurements enabled fairly short term temperature and strain events to be monitored. There were five major air temperature cycles from 23 November 1982 through 13 April 1983 as defined by significant variations

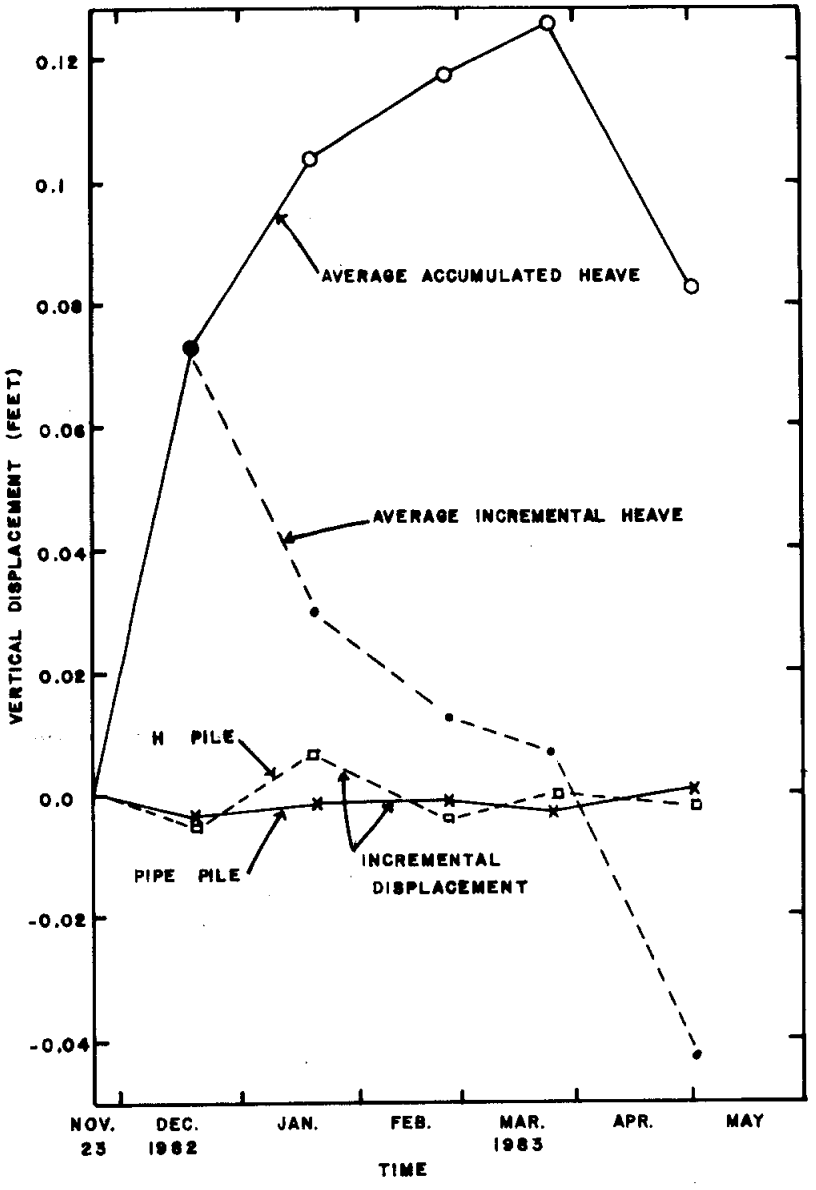

Figure 13. Average incremental and accumulated soil surface vertical heave and incremental vertical displacement for the H- and pipe piles.

in the ground temperature profile at depth (Figure 14). Relatively low temperatures occurred from approximately 23 November to 28 November, 2 December to 6 December, 16 December to 26 December, 2 January to 14 January and from 10 February to 21 February. Short term temperature fluctuations of less than two days duration were superimposed on the major temperature cycles. Diurnal near surface soil temperature fluctuations associated with air temperature fluctuations became noticeable beginning in February. Generally, the very short term fluctuations were not propagated into the soil to any great depth (less than 10 inches). However, some of the longer (greater than one day) fluctuations were reflected in the soil temperature profiles. The temperature distribution along the length of the H and pipe piles was slightly cooler than for the adjacent undisturbed ground. Changes in pile temperatures followed the soil temperature fluctuations closely (Figures 15 and 18). The influence of these temperature fluctuations on the forces (the vertical forces acting on the outer surface of the piles) acting on the H and pipe piles can be readily seen in Figures 16 and 19. The forces, for both piles, in general increased after a decrease in air temperature and decreased after an increase in air temperature. Changes in the forces acting on the piles usually lagged corresponding air temperature changes by a day or more. However, soil temperatures changes at depth were correlated with force changes for short periods of time implying that the lag with air temperature changes were caused by the time required for a temperature wave to propagate to a critical depth within the soil. Soil temperature changes at depth may affect the forces acting on the piles by changing either or both the rate of heave and the adfreeze strength of the soil frozen to the piles. Soil creep deformation mechanisms that reduce the strength of frozen soil would be less active during cold temperature periods and this would result in larger tangential forces acting on the piles. Maximum forces for each pile occurred during the five major temperature cycles, with the largest forces occurring during the 3 January through 14 January cold period. The maximum forces for the pipe and H-pile were 158 kips and 195 kips, respectively.

A mechanism unrelated to the major temperature cycles was also observed to cause changes in the magnitude of forces acting on the piles.

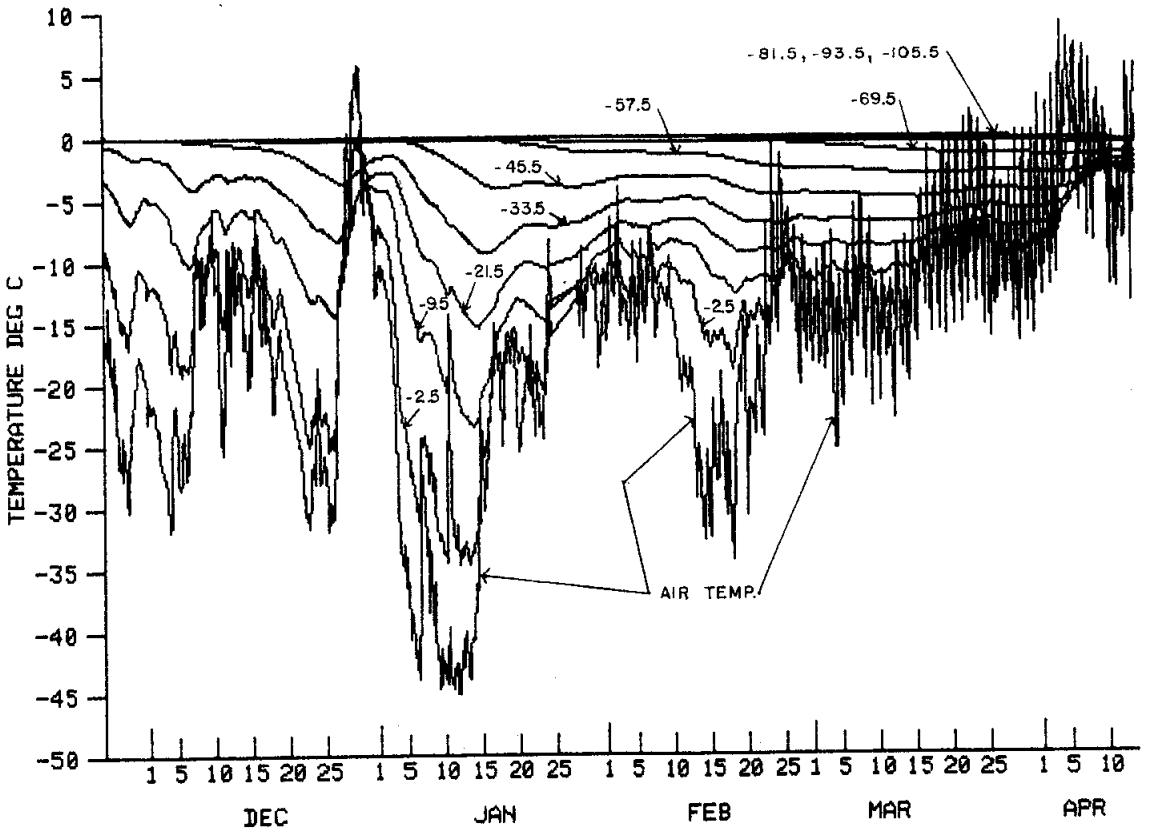

Figure 14. Air temperature and soil temperature at different depths (marked on the figure in inches) for the period 23 Nov 1982 to 13 Apr 1983.

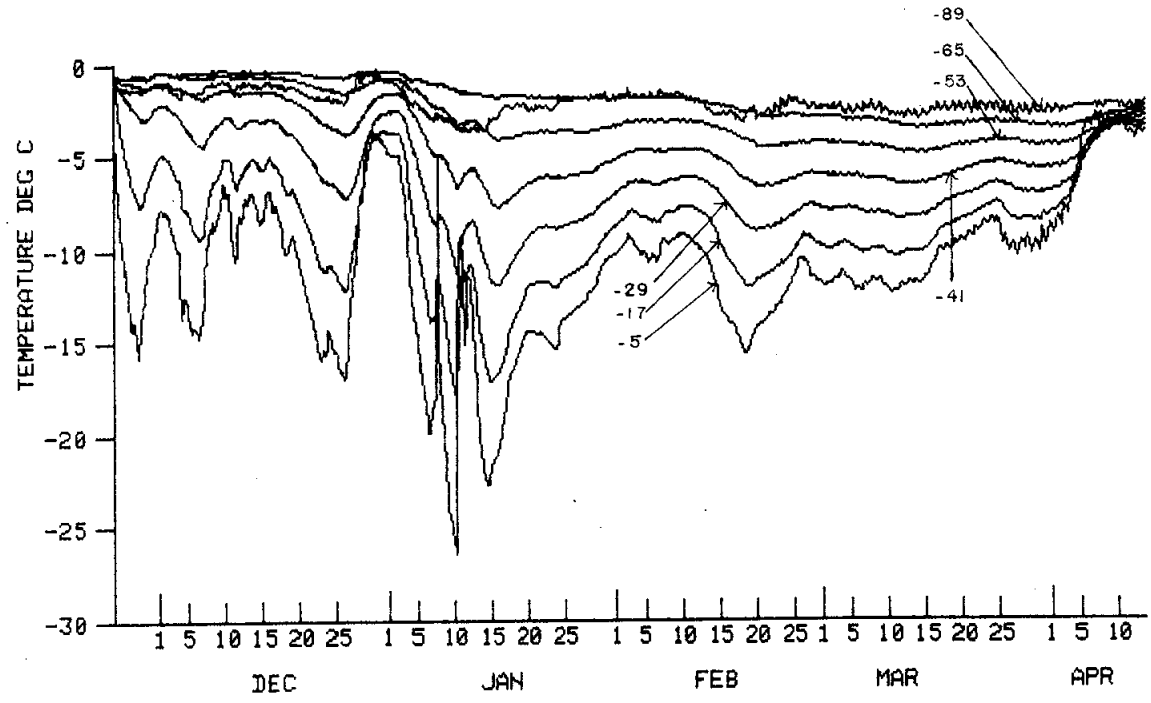

Figure 15. Pipe pile temperatures at different depths (marked on the figure in inches) for the period 23 Nov 1982 to 13 Apr 1983.

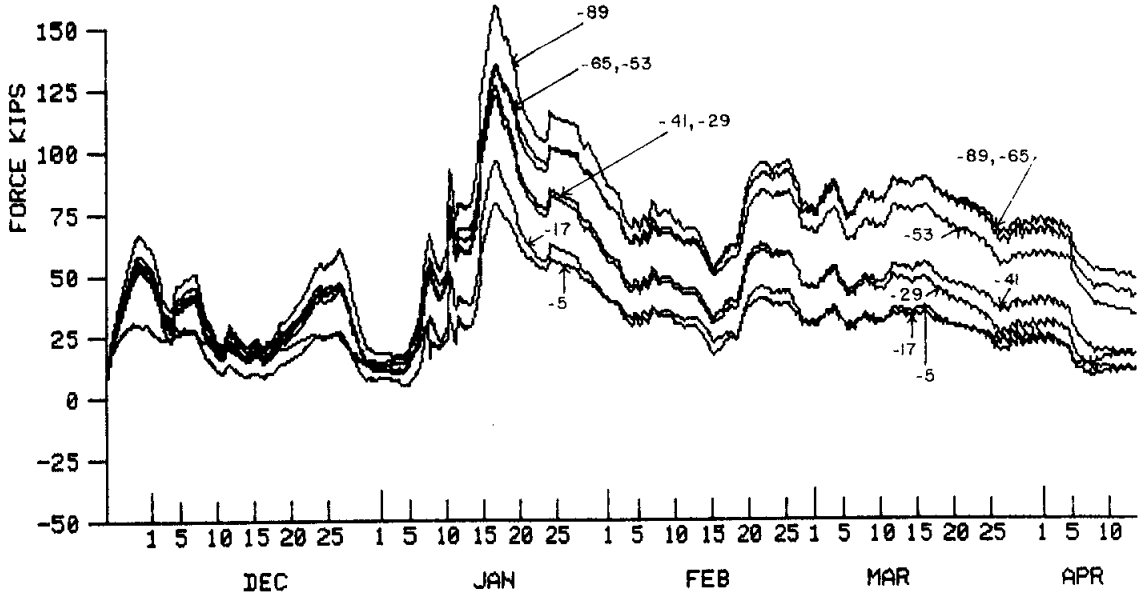

Figure 16. Force for the pipe pile at different depths (marked on the figure in inches) for the period 23 Nov 1982 to 13 Apr 1983.

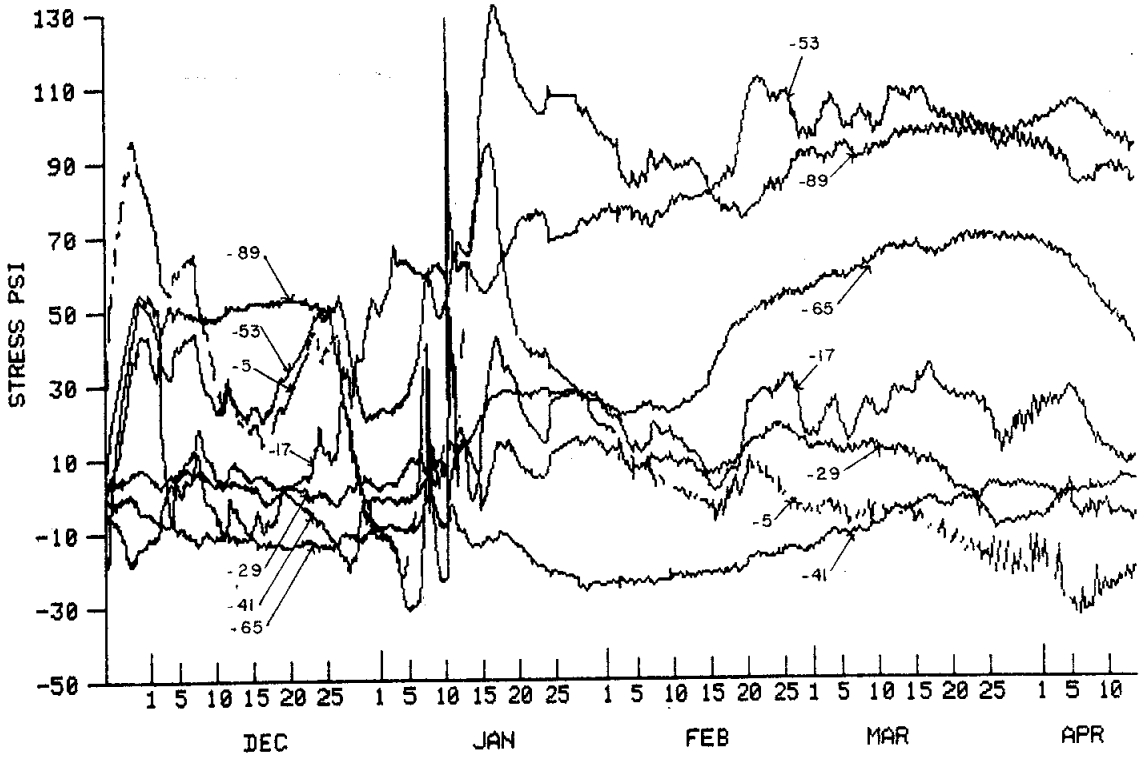

Figure 17. Shear stress for the pipe pile at different depths (marked on the figure in inches) for the period 23 Nov 1982 to 13 Apr 1983.

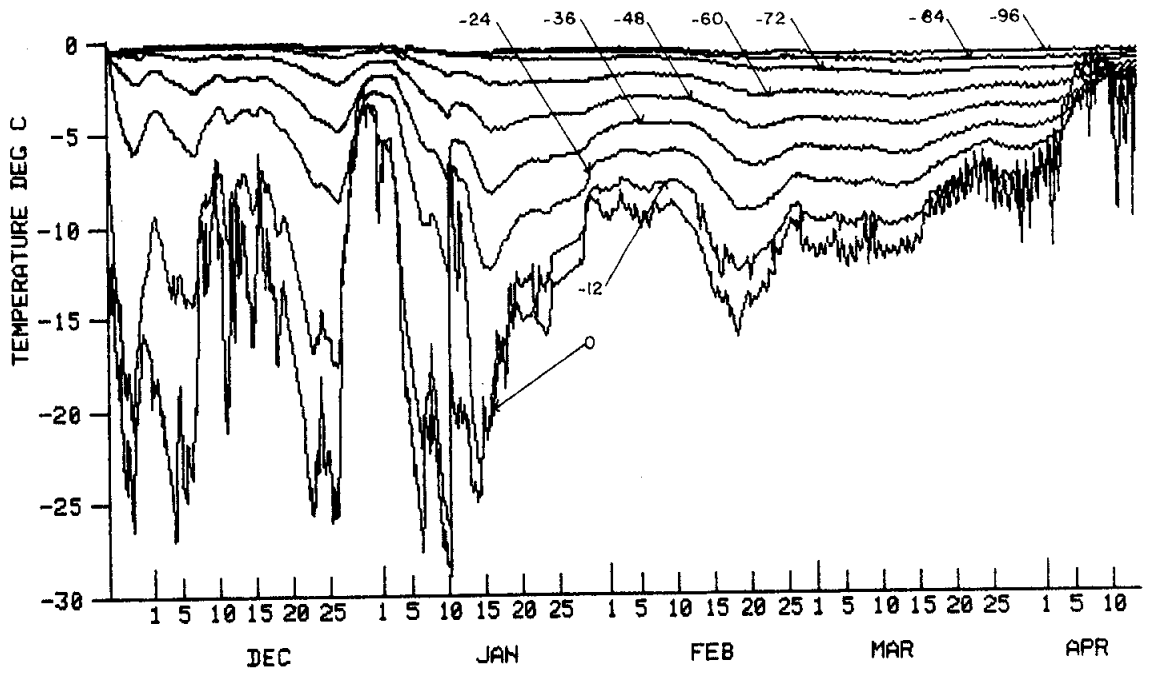

Figure 18. H-pile temperatures at different depths (marked on the figure in inches) for the period 23 Nov 1982 to 13 Apr 1983.

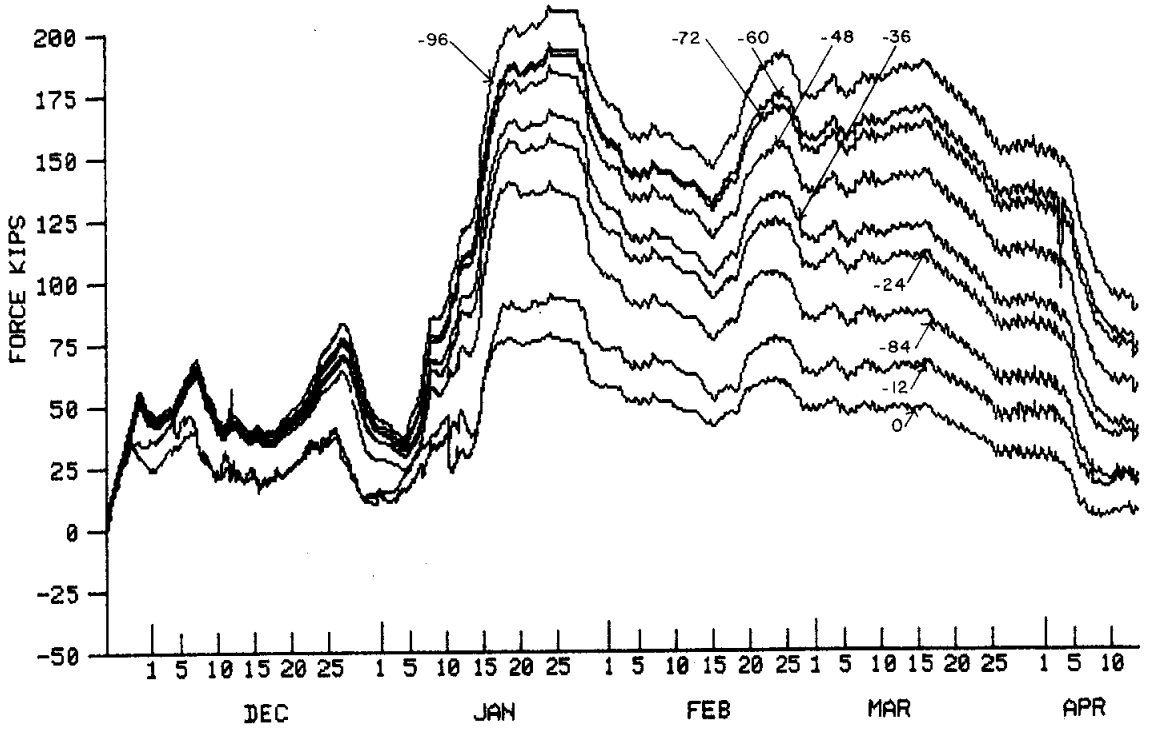

Figure 19. Force for the H-pile at different depths (marked on the figure in inches) for the period 23 Nov 1982 to 13 Apr 1983.

The freezing of water around the H and pipe piles and short term changes in near surface soil temperatures were observed to cause a force that acted along the full length of the instrumented section of the piles. Between 5 January and 13 January, the Alaska Department of Transportation and Public Facilities (DOTPF) used six foot square, ten-inch high wooden forms to freeze water around each pile in an effort to simulate aufeis formation. The water was poured in layers and allowed to freeze, accounting for the sudden temperature spikes seen in Figures 25 and 27. A strong force increase occurred along the full length of the instrumented section of the H and pipe piles immediately following the rise in temperature (Figures 26 and 28). Three mechanisms for causing such a rapid increase in tension in the piles were considered; (1) thermal expansion in the piles reacting against the constraining soil, (2) thermal stresses in the pile caused by strong temperature gradients, (3) volumetric expansion of the upper soil layer due to sudden warming caused by the addition of the water and latent heat of freezing, and (4) volumetric expansion of the ice surrounding the piles during the freezing process (that is as the ice froze it gripped the pile and expanded causing an upward tangential force). Although a quantitative analysis would be required to adequately resolve the problem, the volumetric expansion of upper soil layer and ice were thought to be the dominant mechanisms. The first mechanism was discounted because very little straining would have occurred if the soil constrained the thermal expansion of the piles. The second mechanism was eliminated since the tangential forces increased over the full length of the instrumented section of the piles even though temperature gradients did not vary significantly at the deeper levels. The volumetric expansion concept is consistent with changes in the shear stresses along the length of the pile. Shear stresses are the soil stresses that act on the outer skin of the piles, which may be caused by adfreezing of the soil or soil friction against the pile, and were calculated from the forces. The shear stresses acting on the upper levels of the piles increased in the upward direction while those acting on the lower levels increased in the downward direction (Figures 17 and 20). This

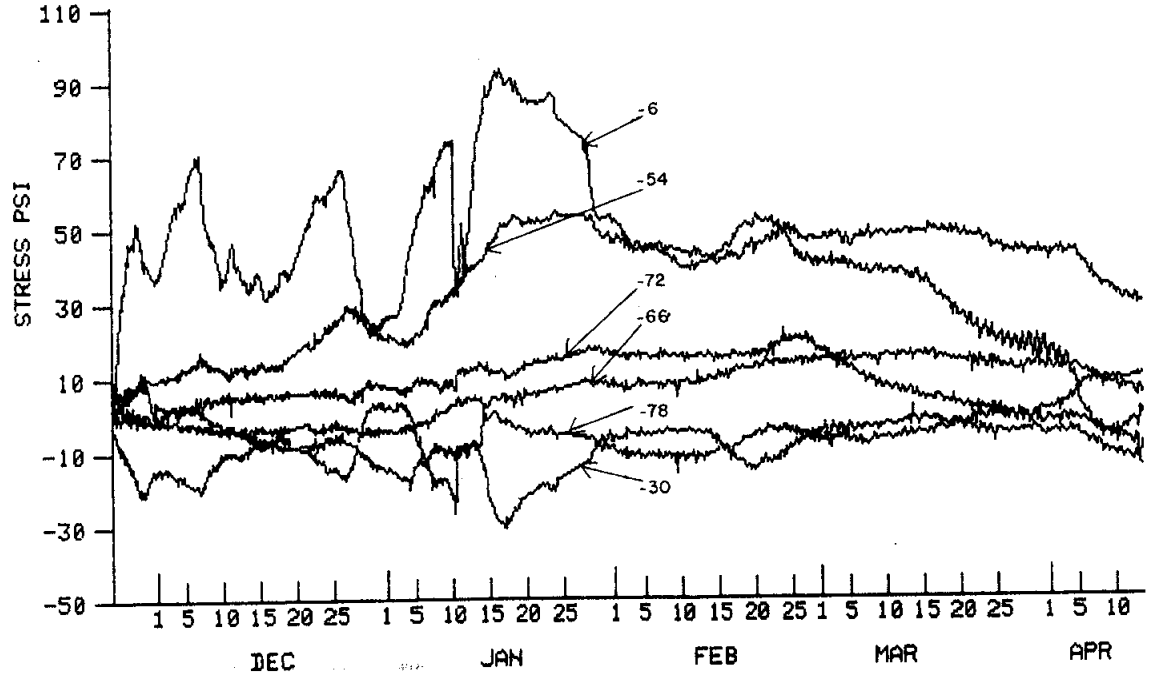

Figure 20. Shear stress for the H-pile at different depths (marked on the figure in inches) for the period 23 Nov 1982 to 13 Apr 1983.

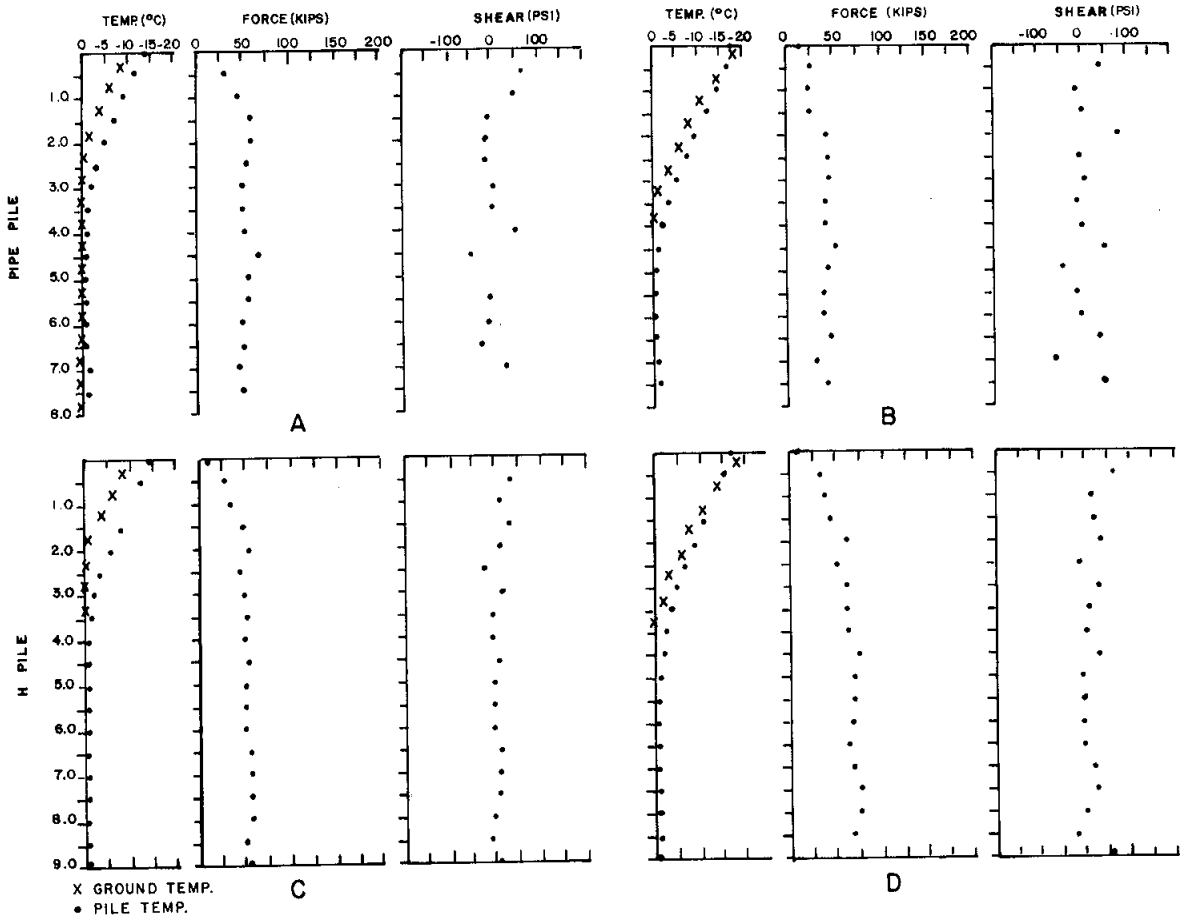

Figure 21. Distribution of relative vertical frost heaving forces and shear stresses over the vertical surface of the pipe and H-piles. Pipe pile: (A) 29 Nov 1982, (B) 25 Dec 1982; H-pile: (C) 29 Nov 1982, (D) 25 Dec 1982.

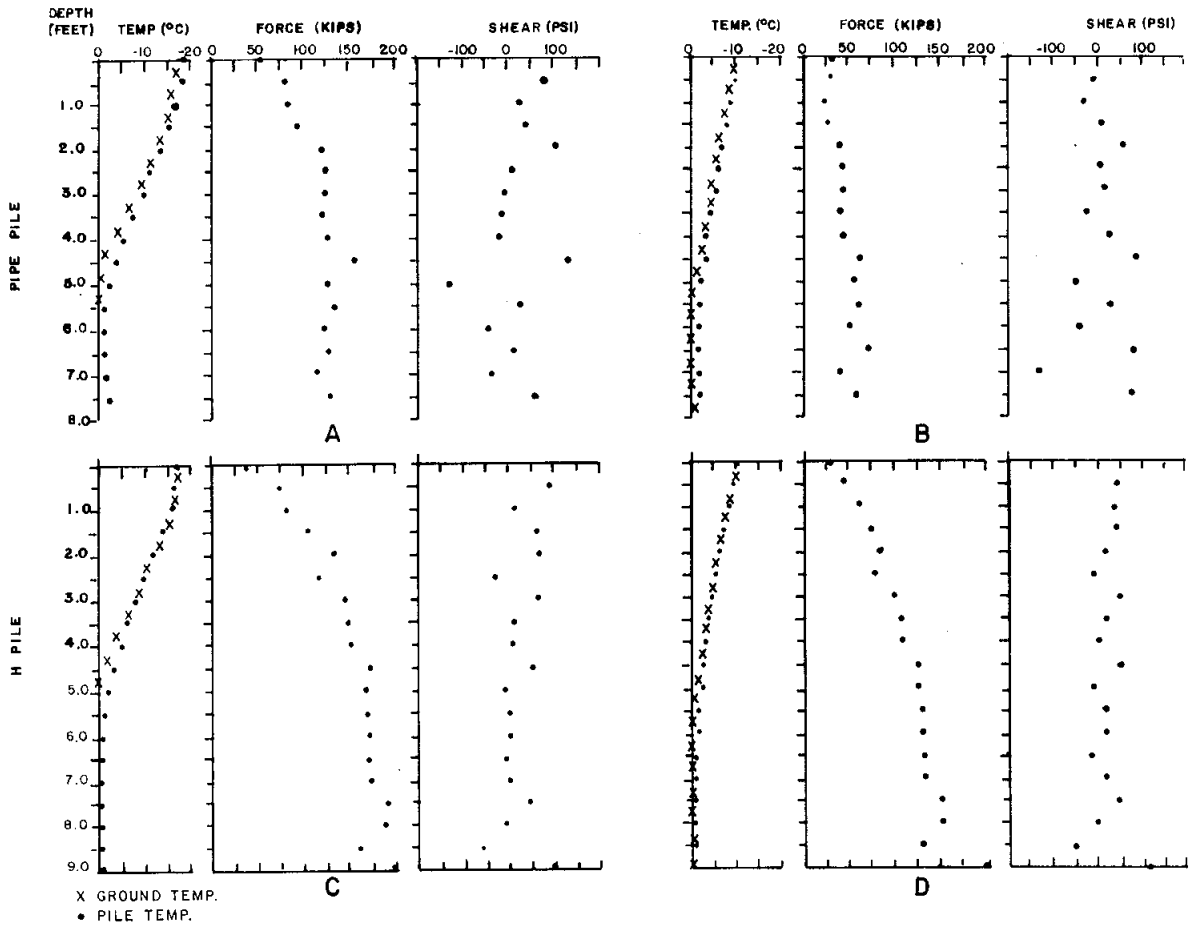

Figure 22. Distribution of relative vertical frost heaving forces and shear stresses over the vertical surface of the pipe and H-piles. Pipe pile: (A) 16 Jan 1983, (B) 12 Feb 1983; H-pile: (C) 16 Jan 1983, (D) 12 Feb 1983.

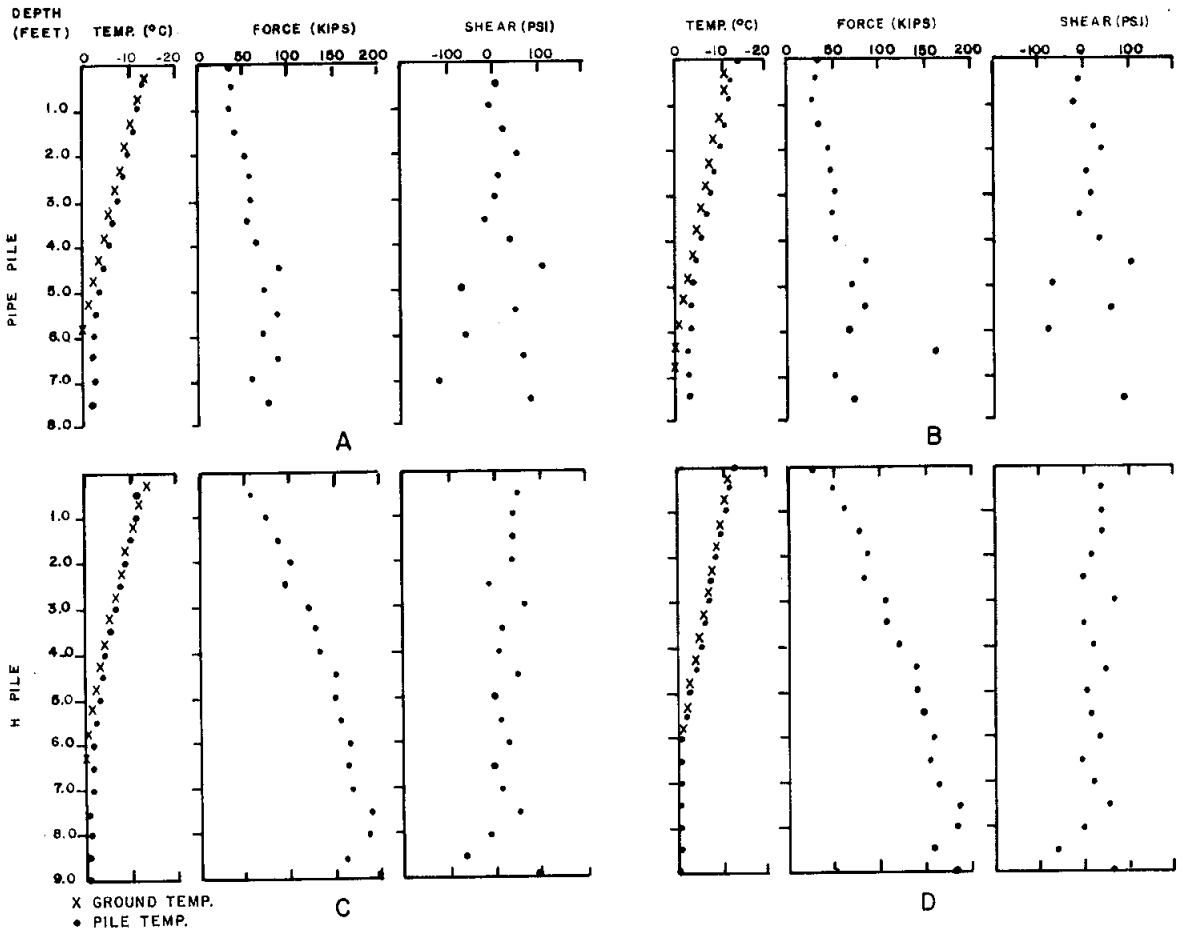

Figure 23. Distribution of relative vertical frost heaving forces and shear stresses over the vertical surface of the pipe and H-piles. Pipe pile: (A) 23 Feb 1983, (B) 11 Mar 1983; H-pile: (C) 23 Feb 1983, (D) 11 Mar 1983.

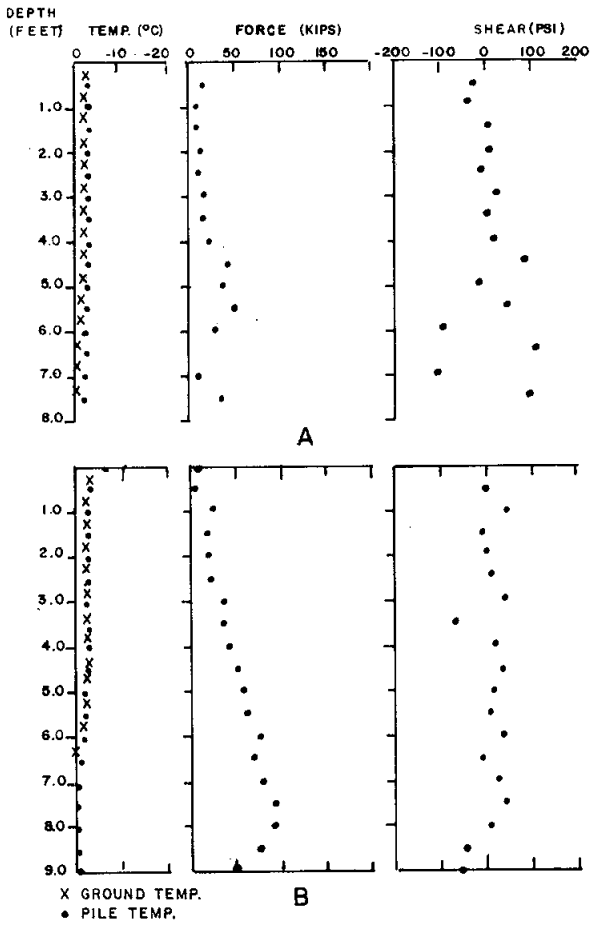

Figure 24. Distribution of relative vertical frost heaving forces and shear stresses over the vertical surface of the pipe and H-piles. Pipe pile: (A) 10 Apr 1983; H-pile: (B) 10 Apr 1983.

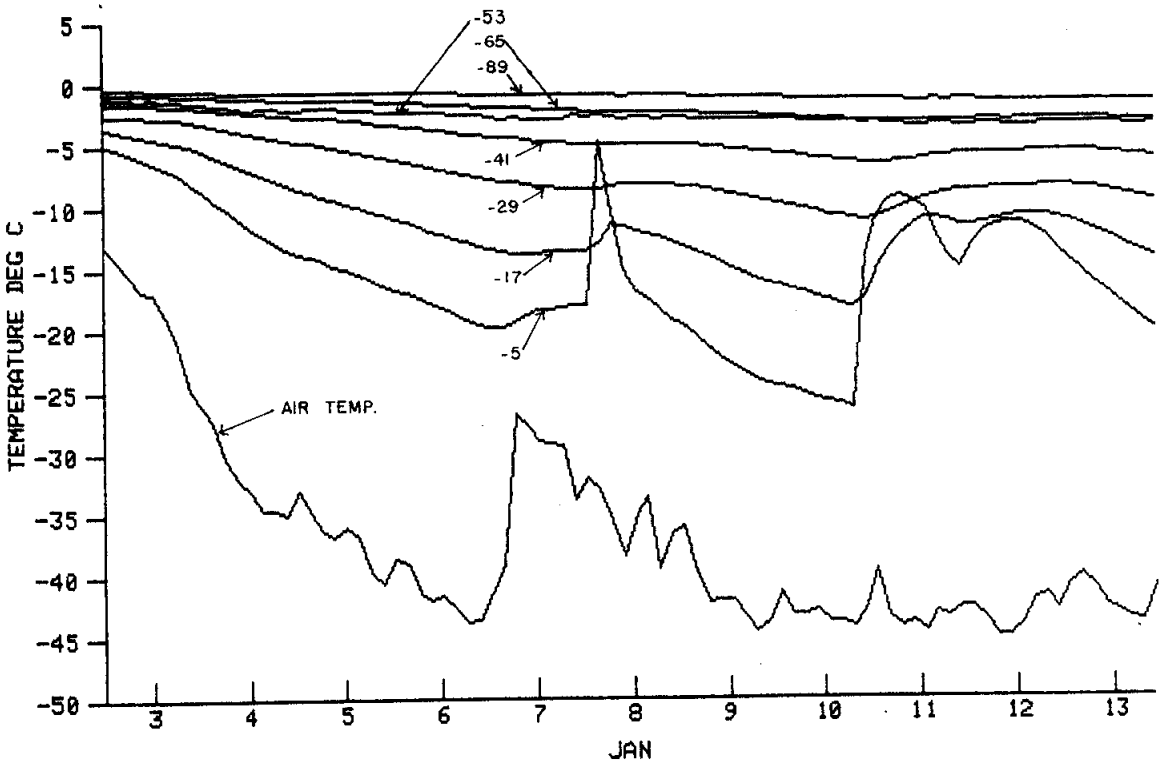

Figure 25. Air temperature and pipe pile temperatures at different depths (marked on the figure in inches) for the period 2 Jan to 13 Jan 1983.

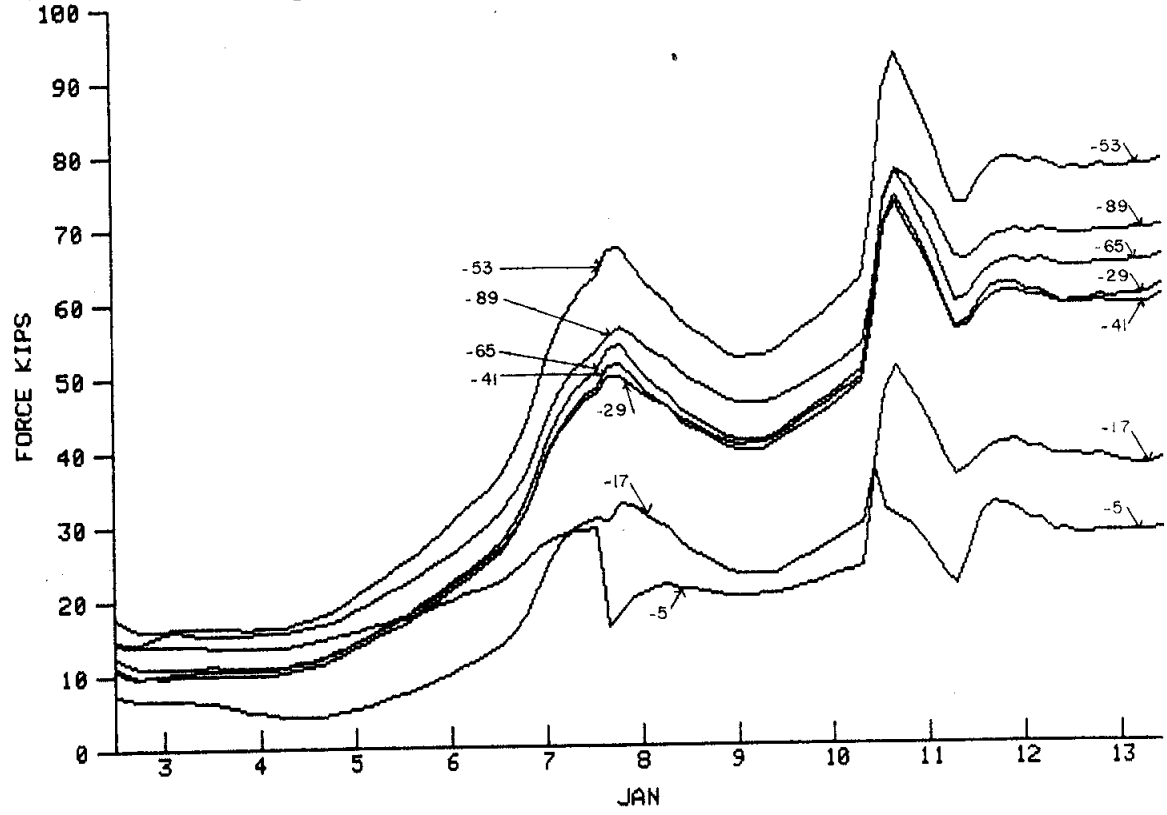

Figure 26. Force for the pipe pile at different depths (marked on the figure in inches) for the period 2 Jan to 13 Jan 1983.

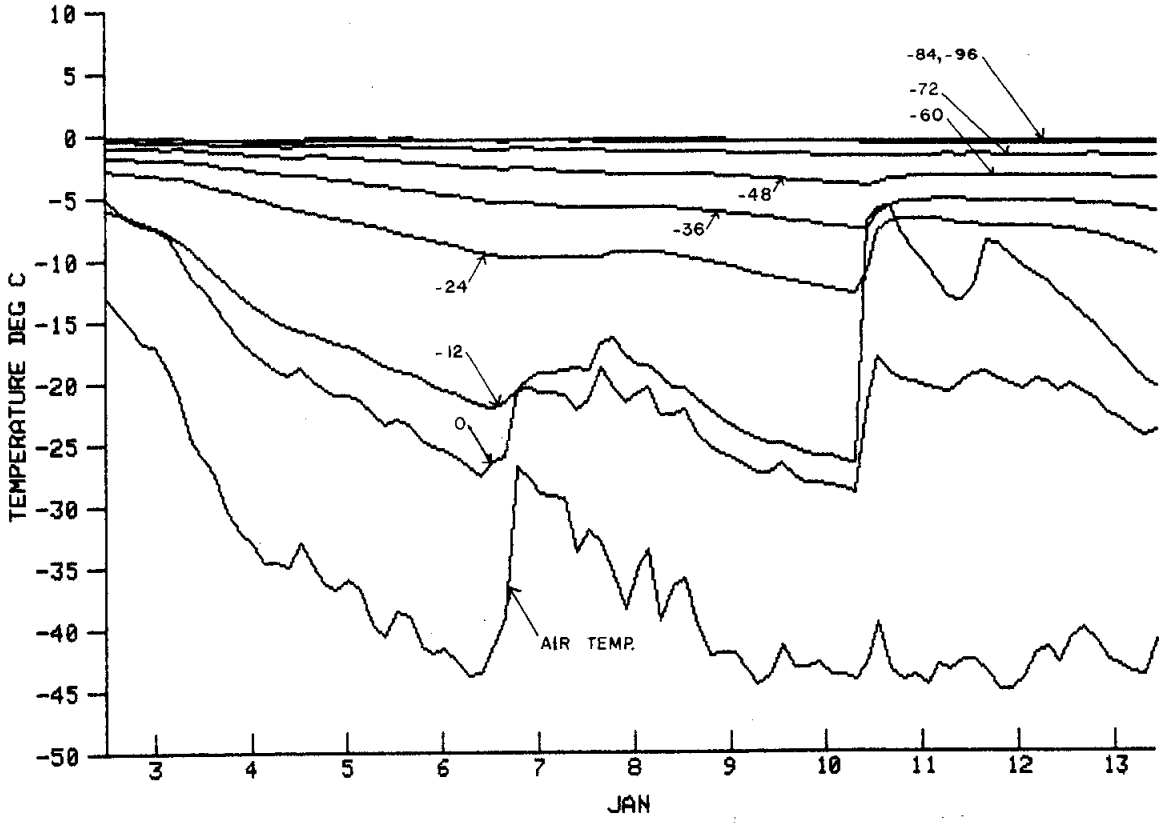

Figure 27. Air temperature and H-pile temperatures at different depths (marked on the figure in inches) for the period 2 Jan to 13 Jan 1983.

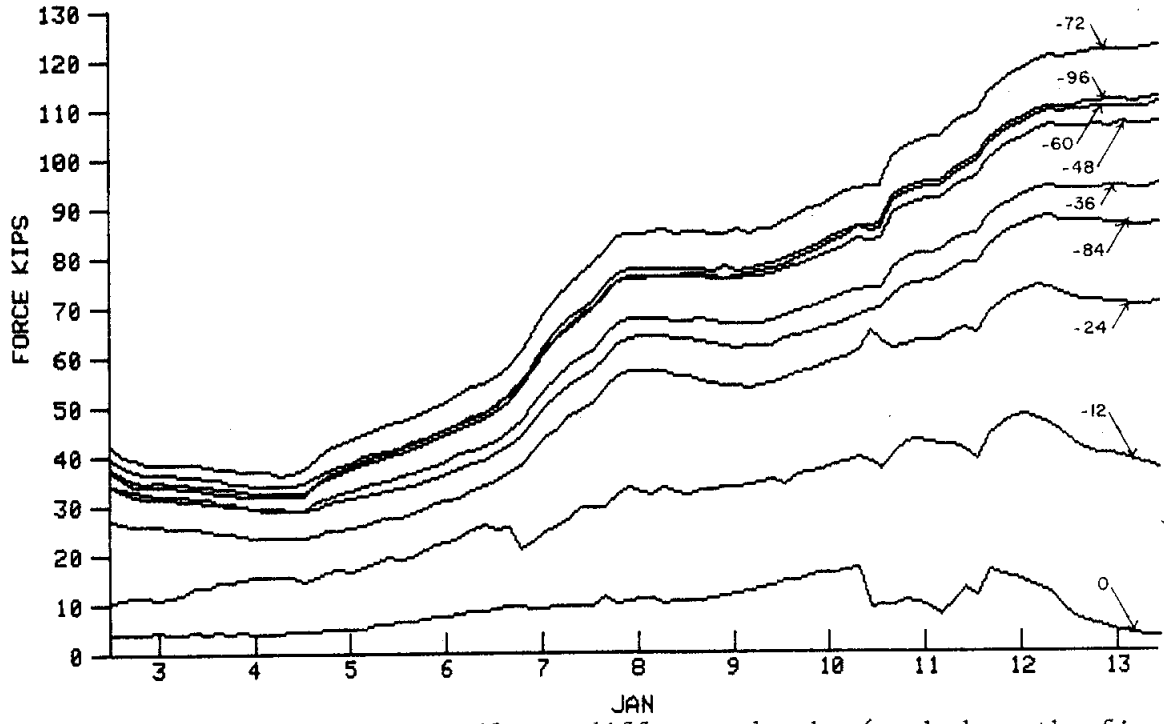

Figure 28. Force for the H-pile at different depths (marked on the figure in inches) for the period 2 Jan to 13 Jan 1983.

would imply that the surface soil layers and the ice block were tending to pull the piles upward against the restraining action of the soil at depth. Creep relaxation may have allowed the forces to relax to a level corresponding to the force trend associated with the major temperature cycle (Figures 26 and 28).

A second set of measurements in March also tend to indicate that volumetric expansion of the soil near the surface caused by temperature changes can create forces in the piles. Diurnal temperature fluctuations from February until the end of the experiment were directly correlated with forces in the piles and are shown for March in Figures 29, 30, 31 and 32. Only the soil layer very near the surface responded to the diurnal fluctuations. The forces acting over the full length of the instrumented sections of the piles tracked the diurnal temperature variations closely. The forces increased with increasing soil temperature near the surface and decreased as soil temperatures decreased.

Shear stresses acting on the H and pipe piles varied in a similar fashion as the forces during the major temperature cycles. The magnitude of the shear stresses increased as air and soil temperatures decreased, and decreased during periods of relatively warm soil temperatures (Figure 17 and 20).

The maximum force and shear stress for the H-pile were 212 psi at a depth of 8 feet and 93 psi on 22 January 1983. The maximum shear stress for the H-pile is 152 psi when the H-pile surface area is computed assuming a rectangular outer boundary. This may be a more realistic stress value since the soil strength along the rectangular boundary is likely to be less than the total adhesion strength of the soil within the pile flanges. The maximum force and shear stress for the pipe pile was 158 kips at a depth of 6.8 ft and 130 psi on 18 January 1983. The average shear stresses for the H and pipe piles, to the depth of the peak forces were 24 psi and 47 psi respectively. The average shear stress for the H-pile was 39 psi assuming a box shaped pile. The magnitude and distribution of shear stress with depth for the piles fluctuated between positive (upwardly directed) and negative (downwardly directed). The stress fluctuations between positive and negative may be a result of not obtaining accurate zeros at the beginning of the study. The actual fluctuations of stress magnitude along the length

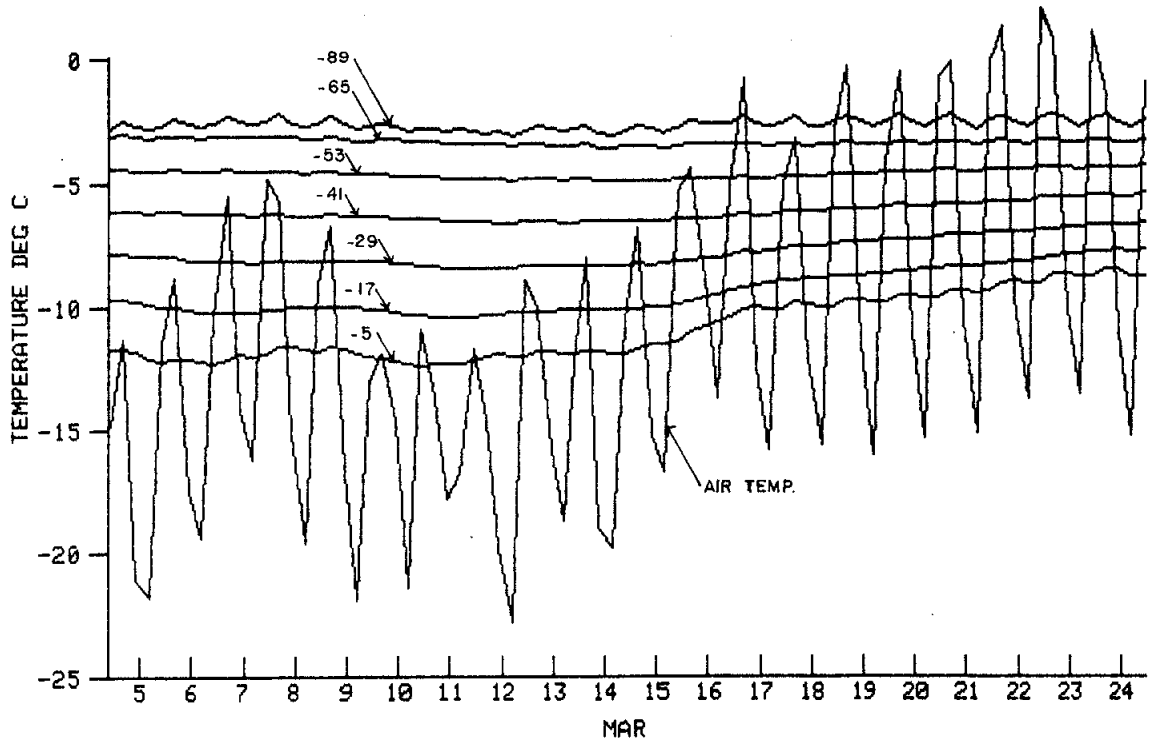

Figure 29. Air temperature and pipe pile temperatures at different depths (marked on the figure in inches) for the period 4 Mar to 24 Mar 1983.

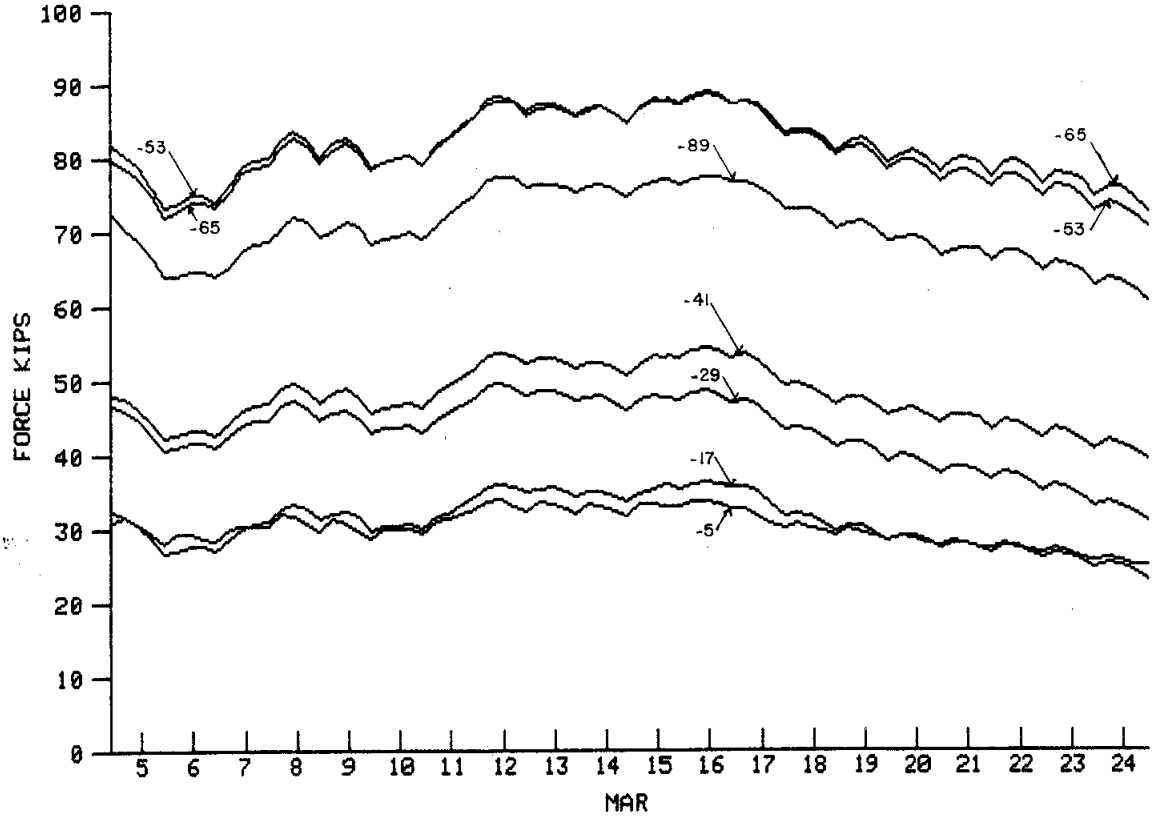

Figure 30. Force for the pipe pile at different depths (marked on the figure in inches) for the period 4 Mar to 24 Mar 1983.

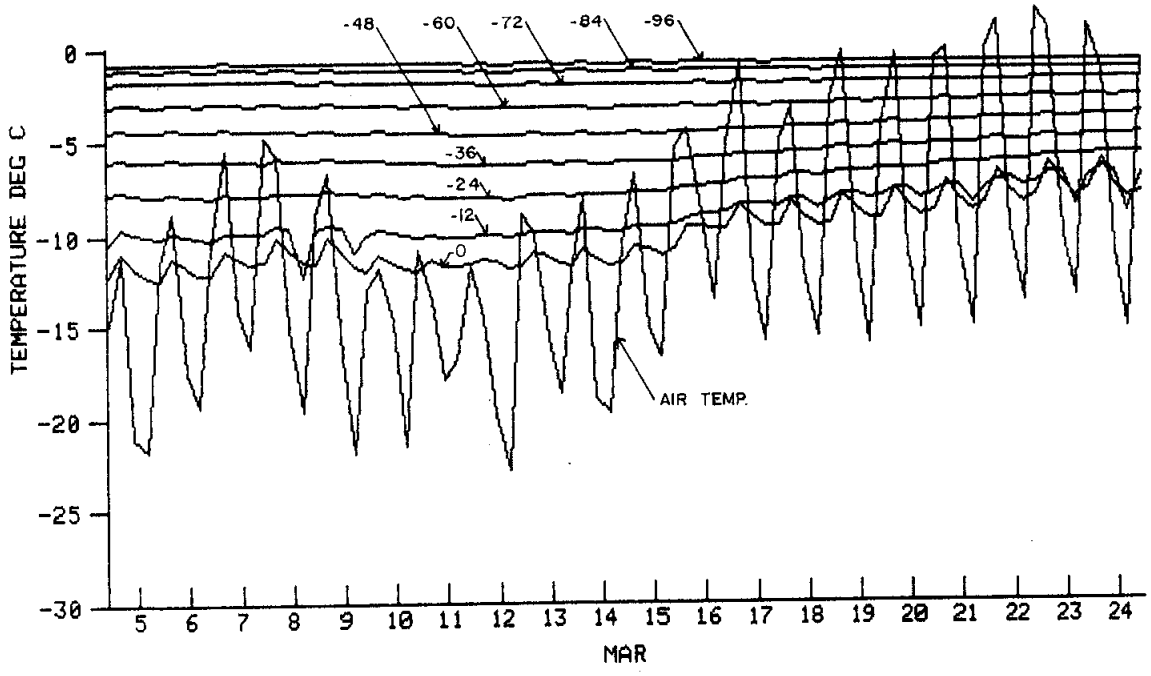

Figure 31. Air temperature and H-pile temperatures at different depths (marked on the figure in inches) for the period 4 Mar to 24 Mar 1983.

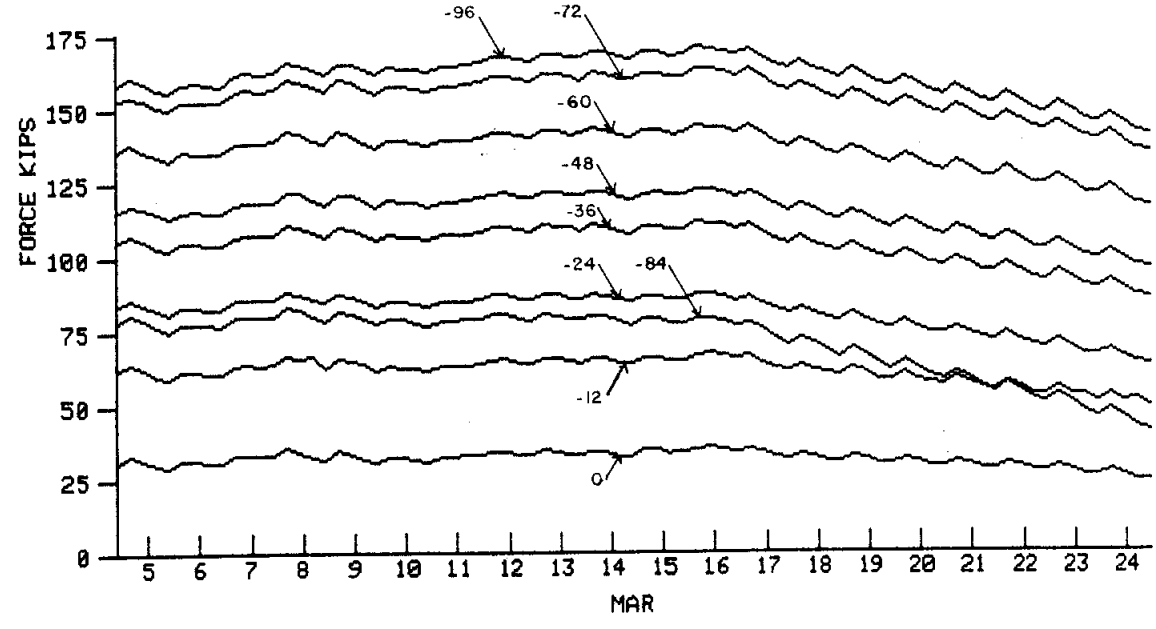

Figure 32. Force for the H-pile at different depths (marked on the figure in inches) for the period 4 Mar to 24 Mar 1983.

of the piles are probably real and are similar to Russian measurements (Tsytovich, 1975). The progression of soil temperatures, H and pipe pile temperatures and force and shear stress distributions for the piles during the winter are shown in Figures 21, 22, 23, and 24.

The freezing of water around the H and pipe piles by Alaska DOTPF in mid-January 1983 was an effort to simulate the effects of aufeis on bridge piles. The forces associated with the freezing water increased by 25 kips for the pipe pile and 12 kips for the H-pile above the ambient force levels associated with soil heave. The addition of the water around the piles occurred during a period of extreme cold. The general level of forces and shear stresses acting on the piles were increasing in response to the cold temperatures. After the water had frozen around the piles the magnitude of forces and shear stresses acting on the piles dropped back to the levels associated with the cold temperatures. This implies that the forces due to freezing the ice blocks around the piles were relieved by creep in the ice and that the long term forces acting on the piles were due to the frozen soil.

BIBLIOGRAPHY

Crory, F.E. and R.E. Reed, 1965. Measurement of frost heaving forces on piles. U.S. Army Cold Regions Res. and Eng. Lab., Technical Report 145, 31 p.

Domashuk, L., 1982. Frost heave forces on embedded structural units. In: Proc. 4th Canadian Permafrost Conference, pp. 487-496.

Johnston, G.H. and B. Ladanyi, 1972. Field studies of grouted rod anchors in permafrost. Can. Geotech. J., 9(2), pp. 176-194.

Kinosita, S., 1967. Heaving force of frozen soils. In: Proc. Int. Conf. Low Temp. Sci. 11, pp. 1345-1360.

Kinosita, S., and T. Ono, 1963. Heaving forces of frozen ground. Mainly on the Results of Field Research. Low Temp. Sci. Lab. Teron Kagaku Ser. A-21, pp. 117-139 (N.R.C. Tech. Transl. 1246, 1966).

Kinosita, S., Y. Suzuki, K. Horiguchi and M. Fukuda, 1978. Observations of frost heaving action in the experimental site, Tomakamai, Japan. In: Proc. 3rd Int. Conf. Permafrost, Vol. 1, pp. 676-678.

Long, E.L., 1972. Method and apparatus for improving bearing strength of piles in permafrost, United States Patent 3, 706, 204.

Penner, E., 1970. Frost heaving forces in Leda Clay. Can. Geotech. J. 7(1), pp. 8-16.

Penner, E., 1972. Influence of freezing rate on frost heaving. Hwy. Res. Bd. Record No. 393, pp. 56-64.

Penner, E., 1974. Uplift forces on foundations in frost heaving soils. Can. Geotech. J., 11(3), pp. 323-338.

Penner, E. and L.W. Gold, 1971. Transfer of heaving forces by adfreezing to columns and foundation walls in frost susceptible soils. Can. Geotech. J., 8(4), pp. 514-526.

Penner, E. and W. W. Irwin, 1969. Adfreezing of Leda Clay to anchored footing columns. Can. Geotech. J., 6(3), pp. 327-337.

Péwé, T.L., 1982. Geologic hazards in the Fairbanks area, Alaska, Special Report 15 Alaska Geological and Geophysical Surveys, 109 p.

Sohlberg, E.T., 1965. Strain gage instrumentation of steel piles in snow, U.S. CRREL TR 152, 30 p.

Sutherland, H.B. and P.N. Gaskins, 1973. Porewater and heaving pressures developed in partially frozen soils. In: Proc. 2nd Int. Conf. Permafrost, North Amer. Contrib., pp. 409-419.

Trow, W.A., 1955. Frost action on small footings. Hwy. Res. Board Bull. No. 100, pp. 22-27.

Tsytovich, N.A., 1975. The mechanics of frozen ground. McGraw-Hill Book Co., pp. 157-162.

Yong, R.N., 1967. On the relationship between partial soil freezing and surface forces. In: Proc. Int. Conf. Low Temp. Sci. II, pp. 1376-1385.

Yong, R.N. and J.C. Osler, 1971. Heaving and heaving pressures in frozen soils. Can. Geotech. J., 8(2), pp. 272-282.

APPENDIX A

Instrumentation and Data Reduction

INSTRUMENTATION AND DATA REDUCTION

Strain Measurements

A Hewlett Packard (HP) 3479A data acquisition/control unit and an HP 85F computer were used to measure the static strains in both the pipe and H-piles. The strain gauges were connected into Wheatstone bridges where one or more of the resistors were active strain gauges (Figure A1a). The voltage ration for a Wheatstone bridge where all the resistors have a fixed value is given by

$$(A1) \qquad (E_o/E)_u = [(R_1)/(R_1+R_4) - R_2/(R_2+R_3)]$$

where E is the excitation voltage to the bridge (5 volts nominally for this experiment), E_o is the output voltage and R_1, R_2, R_3 and R_4 are the resistances of the bridge arms. If the resistance of one of the bridge arms changed, for example, due to straining the arm $(R_4 + \Delta R_4)$, then the voltage ratio would be

$$(A2) \qquad (E_0/E)_s = [R_1/(R_1 + R_4 + \Delta R_4) - R_2/(R_2 + R_3)].$$

The change in the voltage ratio between the strained and unstrained condition is given by

$$(A3) \qquad V_r = [(E_o/E)_s - (E_o/E)_u] = [R_1/(R_1 + R_4 + \Delta R_4) - R_4/(R_1 + R_4)].$$

If $R_1 = R_4$ then

$$(A4) \qquad (-4V_r)/(1 + 2V_r) = (\Delta R_4)/(R_4).$$

The relationship between strain and changes in resistance for resistance strain gauges is

$$(A5) \qquad GF \times \varepsilon = (\Delta R)/(R),$$

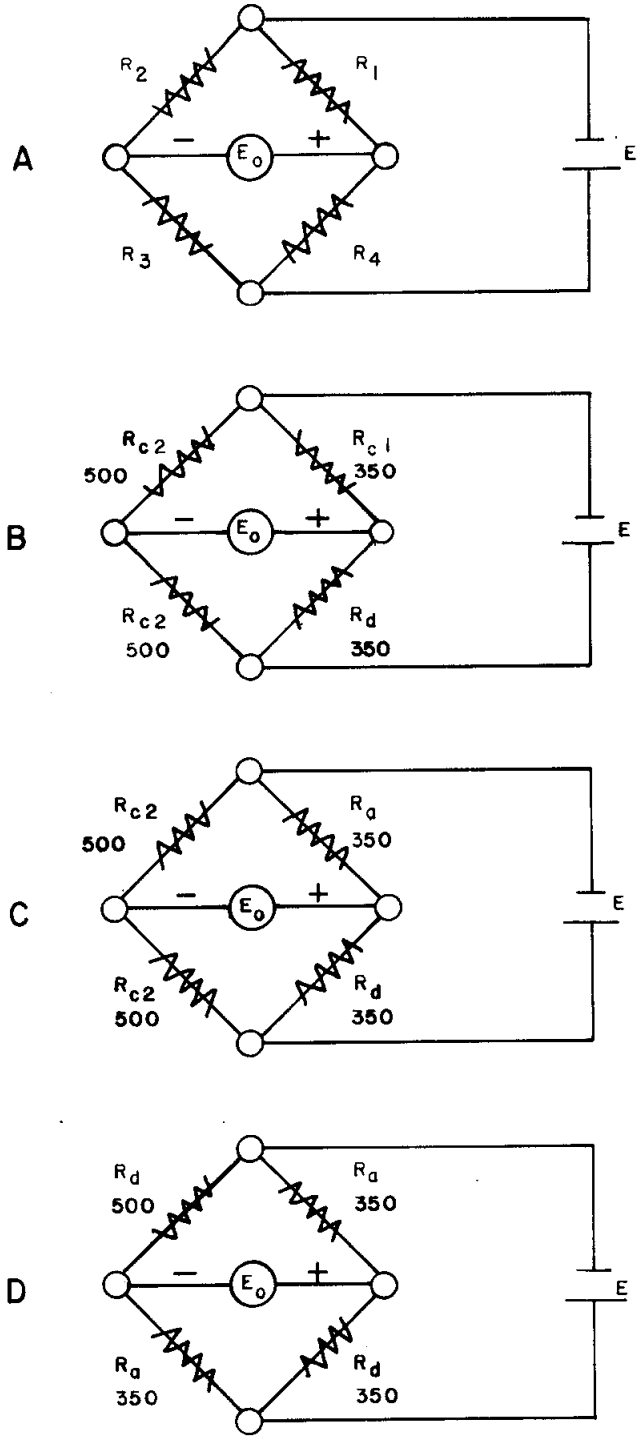

Figure A1. Wheatstone bridge circuits used to measure strain gauge resistance changes. (A) general wheatstone bridge; circuits B, C and D were used to measure one active strain gauge, uniaxial strain with temperature compensated using one active gauge, and uniaxial strain with temperature compensation using two active gauges.

where ε is the strain and GF is the gauge factor determined by manufacturing processes. Strain is positive for positive resistance changes, which occur when the gauge is extended, and can be calculated from

$$(A6) \quad \varepsilon_4 = (-4V_r)/(GF \times (1 + 2V_r)).$$

Equation A6 describes the situation of a Wheatstone bridge where one of the arms is an active strain gauge and the remaining arms of the bridge consist of resistors with fixed values.

In this study three different Wheatstone bridge setups were used with the strain gauges. A single active strain gauge was used to monitor temperature induced apparent strain (Fig. A1b). The gauge was mounted on a shim of metal and attached to the pile so that it remained unstressed. The strain for a single active gauge is given by

$$(A7) \quad \varepsilon_d = (-4V_r)/(GF \times (1 + 2V_r)).$$

Fixed value precision resistors R_{C1} and R_{C2} shown in Figure A1b were used to complete the bridge. These were accessed on the strain gauge multiplexer card that plugs into the backplane of the HP 3497A.

One active strain gauge and one dummy gauge were used in bridges to provide temperature compensation to the strain gauge circuit and to measure uniaxial strain (Figure A1c). The dummy strain gauge, R_d, responds only to thermally induced apparent strains. The active strain gauge, R_a, responds to both thermally and stress induced strains. Thus, the temperature compensated strain for one active gauge connected to a temperature compensating gauge is given by

$$(A8) \quad \varepsilon_a = (4V_r)/(GF \times (1 + 2V_r)).$$

The temperature compensated single active gauge network was only used on the H-pile because symmetric, opposing gauges were not available on each side of the pile web (Figure 8). Space restrictions under the angle necessitated the use of fewer gauges on side 1 of the pile. The single temperature compensated gauges are shown on side 2 in Figure 8 (gauges 16, 19, 21, 23, 26, 28, 31, 33 and 35). The remaining gauges on the H-pile were connected as four arm bridges with two active gauges.

The final Wheatstone bridge setup consisted of four active gauges (Figure A1d). Two of the gauges were for temperature compensation and two gauges were mounted on surfaces that were diametrically opposite from each other in the pipe pile and on opposite sides of the web for the H-pile. The resulting measurement was an average uniaxial strain given by

(A9) $\varepsilon = (2V_r)/(GF \times (1 - 2V_r))$.

Most of the opposing pairs of strain gauges on the pipe pile were connected into Wheatstone bridges with four active arms. The only gauges on the pile that were not connected with four active arms, were gauges 7, 17, 26, 28, 38, 42, 43 and 44. These were connected in separate bridges each with one active gauge (Figure 4).

Although the strain gauges used to measure longitudinal strain were connected so as to reduce errors associated with temperature changes, the gauges did exhibit some temperature sensitivity. This temperature sensitivity was corrected by using apparent strain curves determined from measurements of compensated strain gauges mounted on unstressed locations of the pipe and H-piles (gauges 1 and 21 for the pipe and gauges 1 and 15 for the H-pile). The temperature induced apparent strains were measured over a temperature range of -2°C to -19°C. The apparent strain vs. temperature curve was linear with ε (apparent) = 1.34 per °C with R = 0.987 for the pipe pile and ε (apparent) = 0.999 per °C with R = 0.986 for the H-pile. Corrections for apparent strain were significant only for the upper three strain gauge locations, as temperature changes during the winter were not very great at depth for either pile.

Force and Stress Calculations

After the strain measurements were averaged and corrected for temperature induced apparent strain contributions, the tangential forces and shear stresses acting on the piles were calculated. Several basic assumptions were used in developing the calculation scheme for forces and stresses:

1. Forces acting on the piles were due primarily to vertical shear stresses acting on the surface skin of the pile,

2. Shear stresses along the H and pipe pile surface were the result of frost heaving forces or soil friction and were symetric in the horizontal plane,

3. The stresses acting on the piles in a horizontal plane at any given depth in the soil had azimuthal symmetry.

Figure A2 shows the force diagram for both the pipe and H-piles. A cylindrical coordinate system was used to describe the pipe pile and a Cartesean coordinate system was used for the H-pile.

The above assumptions imply that the stress conditions in the soil acting on the H-pile are given by

$$\text{(A10)} \quad \sigma_x = \sigma_y, \; \sigma_{xz} = \sigma_{yz}$$

The stress-strain relationship for the pile is given by

$$\text{(A11)} \quad \varepsilon_z' = (\sigma_z')/(E) - (\nu)/(E)\,(\sigma_x' + \sigma_y')$$

and

$$\varepsilon_x' = (\sigma_x')/(E) - (\nu)(E)\,(\sigma_y' + \sigma_z'),$$

where ε_z' and ε_x' can be determined from strain gauges mounted on the pile, Young's modulus is E, ν is Poisson's ratio for the pile and σ_x', σ_y', σ_z' are the stresses in the pile acting along the x, y and z coordinate axes. The system of equations (A11) are not solvable in their present form since there are only two equations and three unknowns. If, however, it is assumed that σ_y' in the vicinity of the ε_x' and ε_z' strain gauges is zero, due to the protective angle iron, then the equations become

$$\text{(A12)} \quad \varepsilon_z' = (\sigma_z')/(E) - (\nu\,\sigma_x')/(E) \text{ and}$$

$$\varepsilon_x' = (\sigma_x')/(E) - (\nu\,\sigma_z')/(E).$$

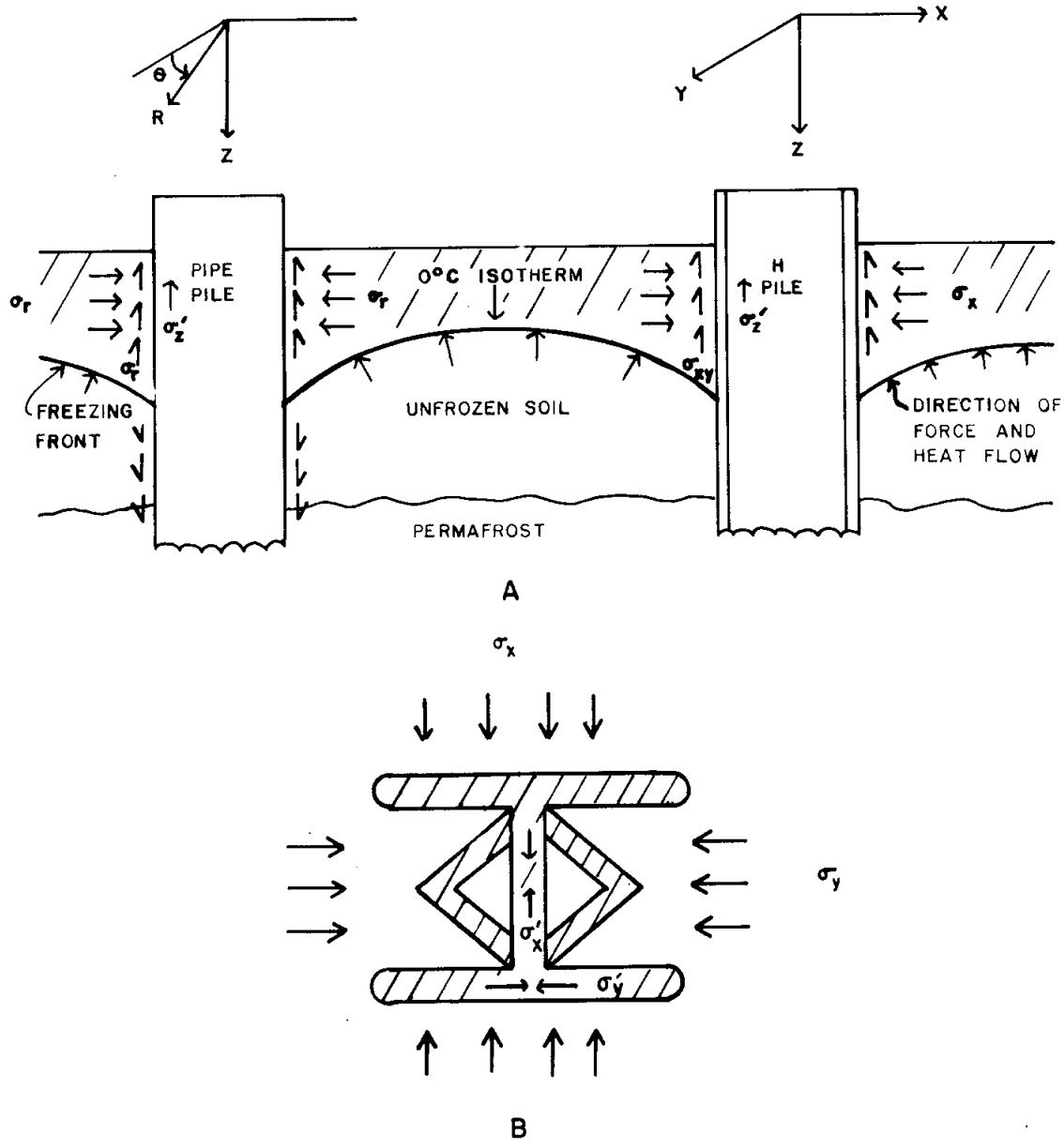

Figure A2. Diagram showing (A) the direction of force and heat flow and (B) the forces acting on the H-pile in the horizontal plane.

Furthermore, the magnitude of transverse stresses, σ_x, is determined by soil confining forces acting against the pile. If these forces are small compared to σ_z', then equation A12 can be simplified. One method of estimating the magnitude of σ_x' is to compare ε_x' to ε_z'. If $\varepsilon_x' \approx -\nu\varepsilon_z$ then the transverse strain is primarily a Poisson's ratio effect caused by σ_z' and σ_x' << σ_z. This result would also imply that σ_y' << σ_z', and the longitudinal stress in the pile can then be given by

$$\sigma_z' = E\varepsilon_z'. \tag{A13}$$

If, however, $\varepsilon_x' > -\nu\varepsilon_x'$ then the longitudinal stress must be calculated using

$$\sigma_z' = E(\varepsilon_z' + \nu\varepsilon_x')/(1-\nu^2). \tag{A14}$$

The strain data for this past winter indicates that $\varepsilon_x' \approx -\nu\varepsilon_z'$ so that equation (A13) was used to calculate stress in the H pile (Figure A3 and A4).

The uplift force acting on the pile was determined from equation A13 by first calculating the axial force on the pile at each strain gauge depth using

$$F_z' = \sigma_z' \times CA_H = E\ \varepsilon_z' \times CA_H. \tag{A15}$$

where CA_H is the cross-sectional area of the H-pile (CA_H = 22.5 in^2). The maximum F_z value corresponds to the total tangential force acting on the pile. The average shear stress acting on the pile was then determined from

$$\sigma_{xz}' = (F_{zi-1}') - F_{zi-1}')/(SA_H \times \Delta z0 \tag{A16}$$

Where SA_H is the surface area of the pile, Δz is the distance between the two strain gauge locations (SA_H = 65.7 in^2), per lineal inch and Δz = 6 inches. The force difference between two adjacent strain gauge depths is given by $(F_{zi} - F_{zi-1})$ where the i^{th} strain gauge location is deeper in the soil than the i^{th}-1 location. This means that σ_{xz} is positive for an upwardly directed shear stress.

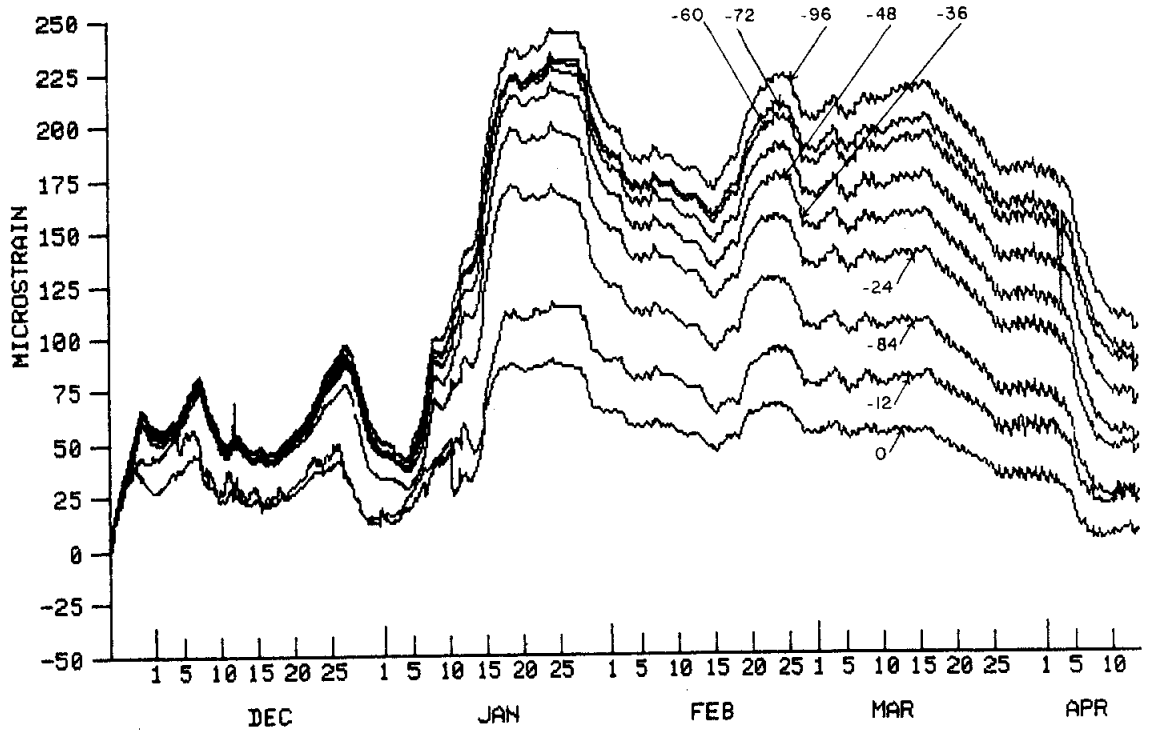

Figure A3. Average longitudinal strain for the H-pile at different depths (marked on the figure in inches) for the period 23 Nov 1982 to 13 Apr 1983.

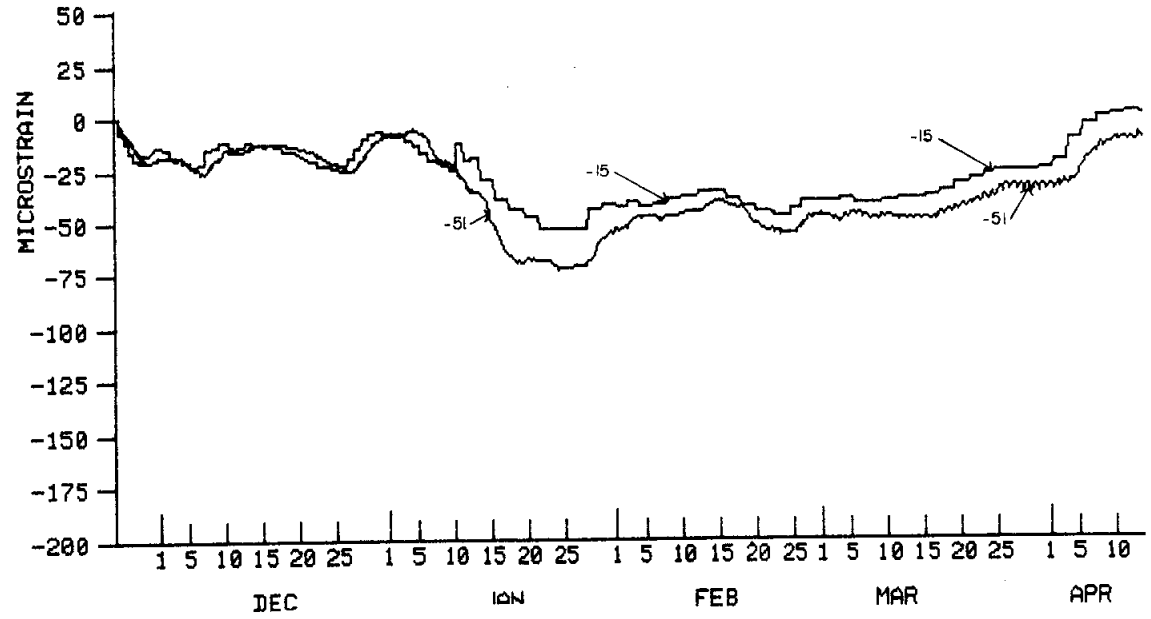

Figure A4. Average transverse strain for the H-pile at depths of 15 in. and 51 in. for the period 23 Nov 1982 to 13 Apr 1983.

Calculating the shear stresses for the pipe pile was done in a similar manner as for the H-pile. The stress conditions along the pipe-soil interface are given, due to the assumptions of the problem, by

$$\sigma_r = \sigma\theta, \text{ and } \sigma_{zr} = \sigma_{z\theta}.$$

The strains for the pipe pile are given by

$$\varepsilon'_\theta = (\sigma'_\theta - \nu\sigma'_z)/E \text{ and}$$

$$\varepsilon'_z = (\sigma'_z - \nu'\sigma_\theta')/E. \quad \text{(A17)}$$

The radial component of stress, σ'_r, is zero since the strain gauges are mounted on a free surface.

Analysis of the full winter's records indicated that, for large magnitude changes in ε'_z, $\varepsilon'_\theta \approx -\nu\varepsilon_z$ (Figures A5 and A6). Therefore $\sigma'_\theta << \sigma'_z$ and the stress in the pipe pile was determined from

$$\sigma'_z = E\varepsilon'_z.$$

The tangential force and shear stresses on the pile were then calculated from

$$F'_x = \sigma'_z \times CA_p$$

$$\sigma_{rz} = (F'_{z_i} - F'_{z_{i-1}})/(SA_p \times \Delta z)$$

Where the cross-sectional area $CA_p = 14.6$ in^2, $SA_p = 40.1$ in^2 per lineal inch is the surface area of the pile and $\Delta z = 6$ inches.

Temperature Measurements

Both thermocouples and thermistors were used to measure temperatures. Thermocouple voltages were referenced against a thermocouple compensation unit built into the HP 3497A multiplexer card. The compensated voltages

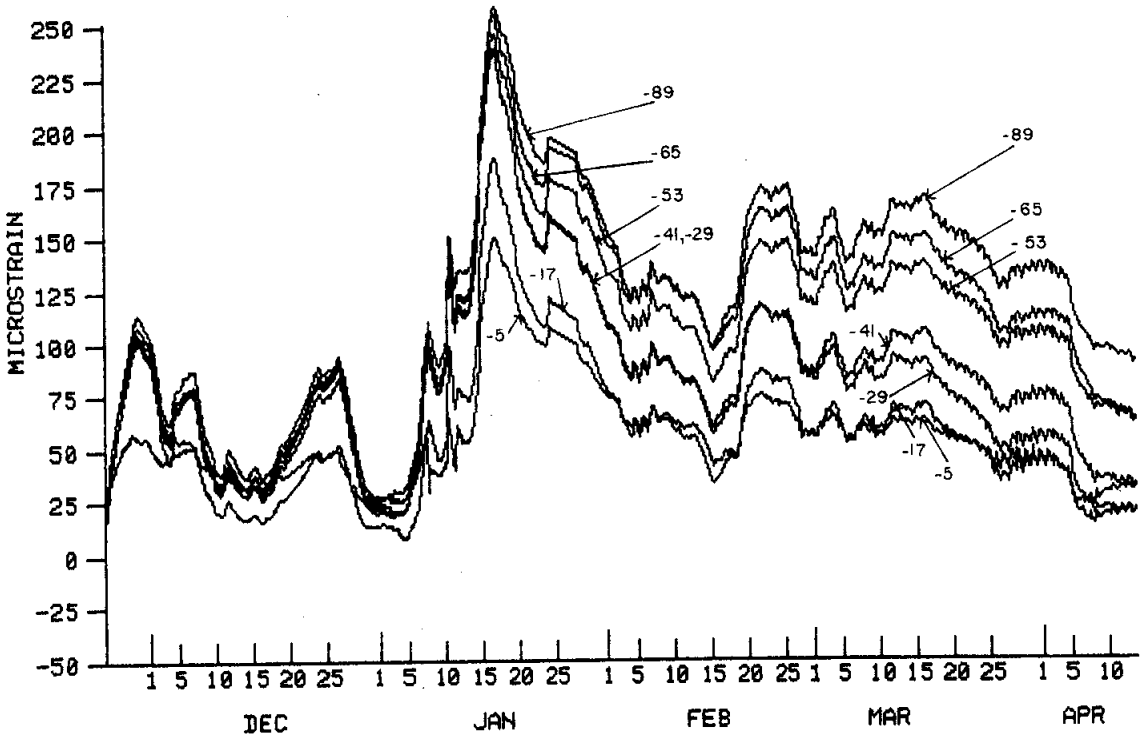

Figure A5. Average longitudinal strain for the pipe pile at different depths (marked on the figure in inches) for the period 23 Nov 1982 to 13 Apr 1983.

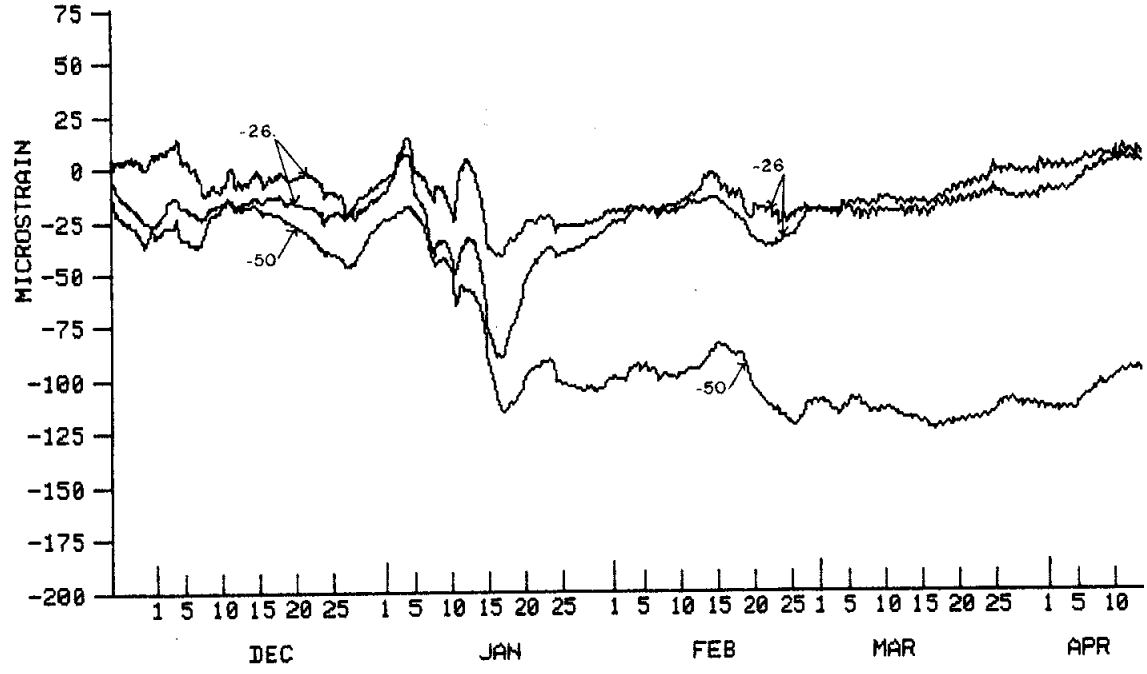

Figure A6. Average hoop strain for the pipe pile at depths of 26 in. and 50 in. for the period 23 Nov 1982 to 13 Apr 1983.

were converted to degrees celsius using the HP85A computer/controller and outputed to a storage tape. The resistance of the thermistors was measured using a 10 μ amp constant current source provided by the HP 3497A, which was activated only during the measurement period. Each thermistor was calibrated at the freezing point prior to their installation. The 0°C thermistor resistance data was then used to adjust the manufacture's calibration curve for the thermistors. The temperature in degrees Kelvin was calculated from

$$(A20) \qquad 1/T = A + B(\ln R) + C(\ln R)^3$$

Where T is degrees Kelvin, R is the thermistor resistance. A, B and C are coefficients that are calculated from the corrected calibration curve for each thermistor;

$$A = y_1 - Bx_1 - Cx_1^3,$$

$$(A21) \qquad B = \frac{(x_1^3 - x_3^3)(y_1 - y_2) - (y_1 - y_3)(x_1^3 - x_2^3)}{(x_1 - x_2)(x_1^3 - x_3^3) - (x_1 - x_3)(x_1^3 - x_2^3)}$$

$$C = \frac{(x_1 - x_3)(y_1 - y_2) - (x_1 - x_2)(y_1 - y_3)}{(x_1 - x_3)(x_1^3 - x_2^3) - (x_1^3 - x_3^3)(x_1 - x_2)}$$

where $y_1 = 1/T$, $y_2 = 1/T_2$, $y_3 = 1/T_3$, $x_1 = \ln R_1$, $x_2 = \ln R_2$ and $x_3 = \ln R_3$. For this study the corrected resistances R_1, R_2 and R_3 for three temperatures 273.15°K, 268.15°K and 263.15°C were used to calculate the A, B and C coefficients for each thermistor. Equation A20 was then used to calculate soil temperatures from the thermistor data.

APPENDIX B

Calibration Test Results for the Pipe Pile and H-Pile

CALIBRATION TEST RESULTS FOR THE PIPE AND H-PILE

Both the pipe and H-piles were calibrated in compression from 0 lbs to 10,000 lbs. The calibration tests were conducted to examine the response characteristics of the strain gauges and to determine an effective Young's modulus and Poisson's ratio for each pile. A reaction beam loading device consisting of a 10,000 lb hydraulic cylinder, 10,000 lb calibrated load cell and loading plattens constrained by four 3/4 inch steel rods was used to load both the pipe and H-piles. The pipe pile was continuously supported along its length and the H-pile was supported every 12 inches during the loading tests. Figure B1 shows the loading frame and data acquisition system used in calibrating the piles.

A linear least squares fit was used to establish the relationship between stress and strain from the load-strain measurements. Figures B2 and B3 show representative plots of the stress-strain data and the best fit line. Figure B2 shows the results from a strain gauge that responded very linearly while Figure B3 shows the results from a malfunctioning gauge. The correlation coefficient for the least squares fit to the data from the malfunctioning gauge was fairly high. It is apparent, however, from the data point distribution that the gauge response was not reliable. Therefore, only data sets with correlation coefficients greater than $r = 0.95$ were accepted as functioning. The stress-strain response was also checked by examining the data plots for each gauge. These were very similar to Figure B2 when the correlations for the stress strain relationships were greater than 0.95.

The calibration test results for the pipe and H-piles are summarized in Tables BI and BII. The results for gauges that are listed together, for example, gauges 1 and 21 at 15 inches on the pipe pile, were averaged. This was done primarily because these gauges were connected into a full wheatstone bridge in the field deployment and provided averaged strain data. The column titled slope is simply the slope of the stress strain curve and the correlation coefficients describe the best fit to the equations

$$\sigma = E\varepsilon$$

for longitudinal gauges and

$$\sigma = (E/\nu)$$

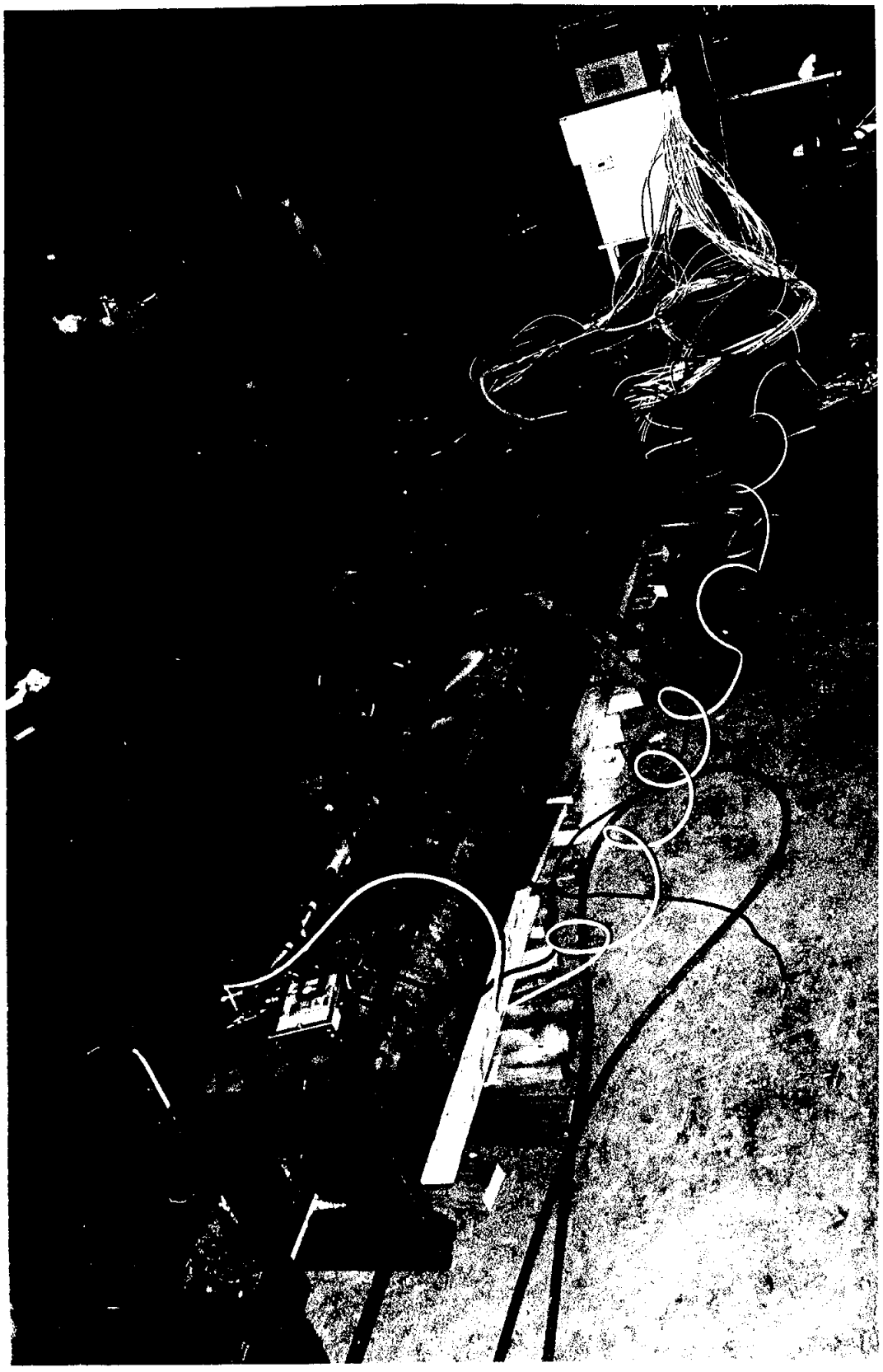

Figure B1. Load frame and data acquisition system for the calibration tests (pipe pile being calibrated).

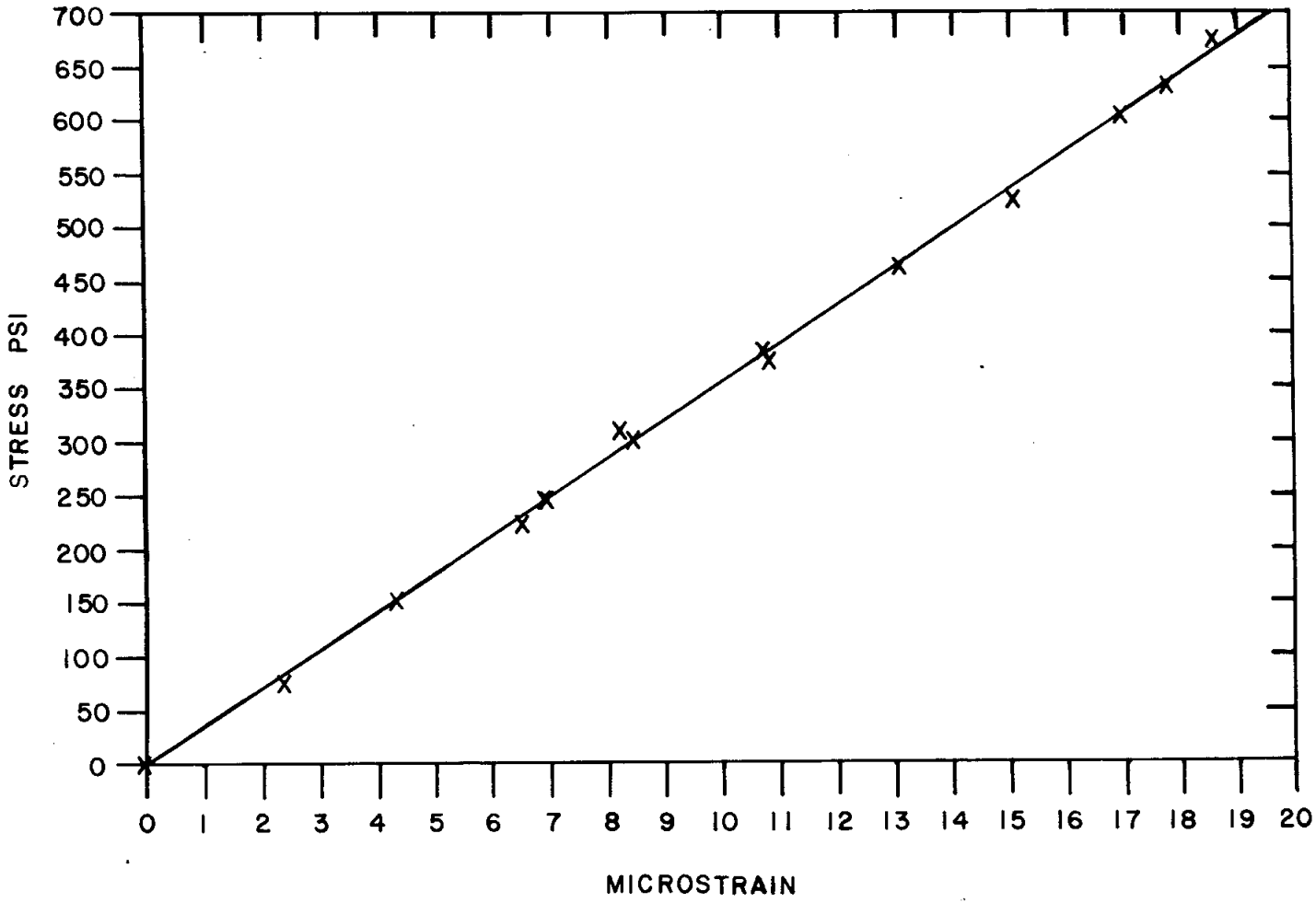

Figure B2. Stress-strain curve for strain gauges 11 and 32 on the pipe pile with correlation coefficient R = 0.999.

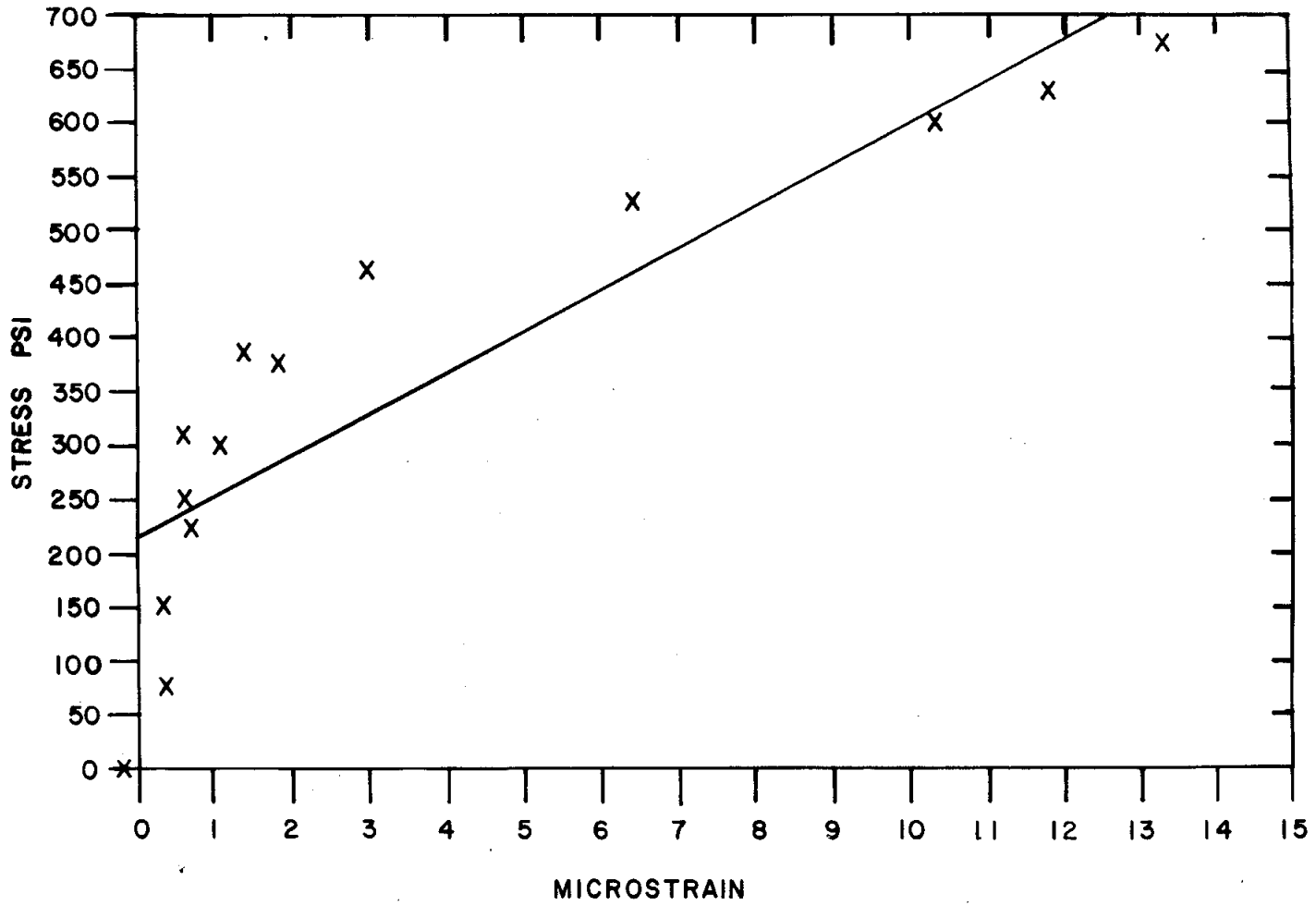

Figure B3. Stress-strain curve for malfunctioning strain gauge 14 on the pipe pile with correlation coefficient R = 0.878.

for transverse gauges, where σ is the applied stress, E is Young's modulus, ν is Poisson's ratio and ε was the measured strain. The calculated effective Young's modulus and Poisson's ratios for the piles are shown in the last column of Tables BI and BII. The effective Young's modulus averaged about 36×10^6 psi for the majority of gauges. This is a somewhat higher value than the published Young's modulus for steel of 30×10^6 psi. The discrepancy may be caused by any of a number of factors including, (1) higher gauge factors for the strain gauge than specifications indicated, (2) errors in calculating the cross-sectional areas for piles, and (3) errors in measuring the applied loads or strains. Variations in the gauge factors are the likely cause since the measured effective moduli are consistent between individual gauges and the two piles. The moduli for two gauge sets on the pipe pile (gauges 6 and 21, 13 and 4) were significantly greater than 36×10^6 psi. These gauges were located within three inches of welded joints and may have been affected by the welding or stress concentrations around the weld joint.

The effective Poisson's ratio for the pipe and H-piles were calculated from a ratio of transverse strain to the average longitudinal strain. The effective Young's modulus values shown in the last column of Tables BI and BII and a Poisson's ratio of 0.33 were used in analyzing the field data.

TABLE BI

Calibration Results for the Pipe Pile

Distance from top of pile in.	Gauge Number	Slope Stress/Strain 10^6 psi	Correlation Coefficient	Youngs' Modulus used in Calculations 10^6 psi
		Longitudinal Gauges		
15	1 & 21	44.5	0.998	36.0
21	2 & 22	38.2	0.999	36.0
27	4 & 24	37.8	0.999	36.0
33	5 7 25	34.5	0.999	35.0
39	6 & 27	40.7	0.999	41.0
45	8 & 29	35.7	0.999	36.0
51	9 & 30	34.9	1.0	35.0
57	10 & 31	35.3	0.999	35.0
63	11 & 32	35.6	0.999	36.0
69	13 & 34	43.7	0.991	44.0
75	14*	38.6	0.878	--
--	35*	371.5	0.919	--
81	15 & 36	--	--	36.0
87	16 & 37	--	--	36.0
93	18 & 39	--	--	36.0
99	19 & 40	34.8	0.999	35.0
105	20 & 41	34.9	0.999	35.0

TABLE BI
(Continued)

Calibration Results for the Pipe Pile

Distance from top of pile in.	Gauge Number	Slope Stress/Strain 10^6 psi	Correlation Coefficient	Poisson's Ratio
		Transverse Gauges		
24	3*	347.4	0.687	--
	23*	253.4	0.836	--
66	12*	32.4	0.82	--
	33*	32.3	0.74	--
74	17	90.3	0.997	.40
	38	86.7	0.997	.42

* malfunctioning gauge

TABLE BII

Calibration Results for the H-Pile

Distance from top of pile in.	Gauge Number	Slope Stress/Strain 10^6 psi	Correlation Coefficient	Youngs' Modulus used in Calculations x 10^6 10^6 psi
		Longitudinal Gauges		
99	11	35.9	0.997	37.0
--	32	38.8	0.998	--
105	33	38.9	0.987	39.0
111	12	37.2	0.999	38.0
--	34	38.1	0.994	--
117	35	34.1	0.997	34.0
123	14	32.5	0.997	33.0
--	37	33.2	0.983	--
		Transverse Gauges		Poisson's Ratio
30	3	101.1	0.95	0.36
--	18	76.0	0.947	0.47
66	7	85.6	0.978	0.42
--	25	104.0	0.988	0.35
90	10	110.3	0.966	0.33
	30	92.2	0.991	0.39
120	13	126.4	0.985	0.29
--	36*	20.25	0.991	--

* malfunctioning gauge

TABLE BII
(Continued)

Calibration Results for the H-Pile

Distance from top of pile in.	Gauge Number	Slope Stress/Strain 10^6 psi	Correlation Coefficient	Youngs' Modulus used in Calculations x 10^6 10^6 psi
		Longitudinal Gauges		
15	1	33.0	0.994	32.0
	5	31.8	0.988	--
21	16	38.6	0.988	39.0
27	2	36.8	0.991	36.0
	17	36.0	0.988	--
33	19	35.2	0.988	35.0
39	4	36.8	0.993	36.0
--	20	35.3	0.993	--
45	21	36.4	0.986	36.0
51	5	34.9	0.988	35.0
--	22	35.8	0.993	--
57	23	39.5	0.982	40.0
63	6	34.1	0.994	34.0
--	24	34.7	0.993	--
69	26	36.6	0.993	37.0
75	8	35.2	0.984	36.0
--	27	36.1	0.991	--
81	28	35.2	0.994	35.0
87	9	35.6	0.982	--
93	31	37.3	0.998	37.0